ISSN 0234-5366

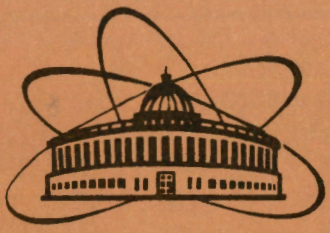

ОБЪЕДИНЕННЫЙ
ИНСТИТУТ
ЯДЕРНЫХ
ИССЛЕДОВАНИЙ

JOINT INSTITUTE
FOR NUCLEAR
RESEARCH

5[56]-92

КРАТКИЕ СООБЩЕНИЯ ОИЯИ

JINR RAPID COMMUNICATIONS

ДУБНА

Объединенный институт ядерных исследований
Joint Institute for Nuclear Research

№5[56]-92

КРАТКИЕ СООБЩЕНИЯ ОИЯИ
JINR RAPID COMMUNICATIONS

сборник
collection

Дубна 1992

ОГЛАВЛЕНИЕ
CONTENTS

УДК 621.039.8.002:621.384.6

ULTRA PURE PLUTONIUM-237. PRODUCTION AND CHARACTERISTICS

Yu.Ts.Oganessian, S.N.Dmitriev, G.V.Buklanov, Yu.P.Kharitonov, A.F.Novgorodov, L.I.Salamatin, G.Ya.Starodub, S.V.Shishkin, Yu.V.Yushkevich

The ^{237}Pu was obtained in the reaction ^{235}U (^{4}He, 2n) at the high-current heavy ion accelerator U-200. ^{235}U of the 99,99% isotopic purity was used as a target. The dependences of ^{236}Pu, ^{237}Pu, ^{238}Pu yields on the energy of the ion beams were studied. Plutonium was isolated from the irradiated target by using the anion-exchange chromatography. An additional isotopic enrichment of the ^{237}Pu was carried out with an electromagnetic mass-separator YASNAPP-2. The preparation obtained with ^{236}Pu/^{237}Pu/^{238}Pu ratio equal to $2.10^{-7}/1/\leq 3.10^{-7}$ (Bq/Bq) is the purest one among the preparations reported to date by different Laboratories. The preparation with the above purity is practically harmless for the volunteer's organism at the metabolism study *in vivo*.

The investigation has been performed at the Flerov Laboratory of Nuclear Reactions and at the Laboratory of Nuclear Problems, JINR.

Ультрачистый плутоний-237. Получение и характеристики

Ю.Ц.Оганесян и др.

Плутоний-237 получен в реакции ^{235}U (^{4}He, 2n) при облучении мишени из высокообогащенного ^{235}U (99,99%) на высокоточном ускорителе У-200. Исследована зависимость выхода ^{236}Pu, ^{237}Pu, ^{238}Pu от энергии ^{4}He. Выделение плутония из облученной мишени проводилось с использованием анионообменной хроматографии. Дополнительное изотопное обогащение ^{237}Pu проводилось на электромагнитном масс-сепараторе ЯСНАПП-2. Полученный препарат плутония-237 с отношением активностей ^{236}Pu/^{237}Pu/^{238}Pu = $2\cdot10^{-7}/1/3\cdot10^{-7}$ (Bq/Bq) является существенно более чистым по сравнению с аналогичными препаратами, произведенными в других лабораториях. Препарат указанной чистоты является практически безопасным для организма человека при проведении исследований метаболизма плутония in vivo.

Работа выполнена в Лаборатории ядерных реакций имени Г.Н.Флерова и в Лаборатории ядерных проблем ОИЯИ.

The considerable interest to the problem of the production of ^{237}Pu is based on the fact that it is the only Pu isotope which answers the medical requirements to the metabolism research *in vivo*. A ^{237}Pu preparation used for injection to human body must be substantially free from alpha-emitting plutonium isotopes. Some works have reported on the methods of preparing ^{237}Pu in the following reactions: ^{235}U, (^{4}He, 2n) [1—4], ^{238}U (^{4}He, 4n) [5], ^{235}U (^{3}He, n) and ^{238}U (^{3}He, 4n) [6,7]. The purest ^{237}Pu preparation was obtained by Pelevin et al. [4] at irradiating an enriched ^{235}U (99,99%) target with alpha-particles of 24 MeV at the cyclotron U 200 of FLNR. The ratios of the Pu isotopes activity (Bq/Bq) in this preparation were $1.7 \cdot 10^{-5}$ ($^{236}Pu/^{237}Pu$) and $1.1 \cdot 10^{-4}$ ($^{238}Pu/^{237}Pu$). That was a high, but insufficient purity. The calculated committed effective doses (mSv/kBq) for Pu isotopes are: 182 (^{236}Pu), 0.001 (^{237}Pu), 504 (^{238}Pu) [8], i.e. 1 kBq of the above preparation has about 0.060 mSv, from which ^{237}Pu gives only 1.5%.

The main goal of this work was the elaboration of the method of producing a radiochemically and isotopically ultra pure ^{237}Pu preparation. A simple calculation shows that the ratios of the activities of ^{236}Pu and ^{238}Pu to that of the ^{237}Pu must be less than 10^{-6} for the effective dose of the Pu preparation to be formed in the main by the ^{237}Pu. To achieve this goal the optimal irradiation conditions were determined and an additional enrichment of ^{237}Pu with a mass-separator was used. The initial ^{237}Pu preparation was produced in ^{235}U (^{4}He, 2n) reaction with an enriched ^{235}Pu (99,993%) target at the cyclotron U-200.

Experimental

Target preparation and irradiation. The isotopically enriched ^{235}U(99,993%) as an oxide was converted to a nitrate form. The uranyl nitrate was spread on the aluminium target block with the cylindrical surface, which was then heated to convert the uranium to the oxide form. The thickness of the uranium targets was 1.0 (eight targets) and 5.0 $mg.cm^{-2}$. The ^{235}U targets were irradiated in the inner channel of the cyclotron U-200 at the ^{4}He-ions energy from 22.0 up to 26.5 MeV.

Isolation of Pu from the target. After cooling for 3 days, the irradiated uranium targets on aluminium backings were dissolved from the backings with the 12 M nitric acid. Plutonium was then reduced to Pu(IV) with a sodium nitrite and the preliminary separation of Pu(IV) from uranium

was carried out by the lanthanium fluorid method. The sediment was dissolved with the 7.5 M HNO_3 – 0.1 M $NaNO_2$ solution and the solution containing Pu(IV) was introduced into the anion exchange column filled with the Dowex 1 × 8 200/400 mesh resin. The residual uranium, the activation and the fission products were eluted from the columns with a large volume of 7.5 M HNO_3 – 0.1 M $NaNO_2$ solution and then with 9.0 M HCl. The plutonium fraction was obtained from the column by elution with the 9.0 M HCl – 0.1 M NH_4I solution. The solution was then evaporated to dryness and burnt on a hot-plate untill the decomposition of ammonium iodide. After that the sediment was dissolved with a small volume of the 7.5 HNO_3 – 0.1 M $KBrO_3$ solution, which was introduced into a microcolumn filled with the Dowex 1×8 200/400 mesh resin. The potassium bromate eluted with 9.0 M HCl and plutonium was then eluted with a small volume (2—3 drops) of 2.0 M HCl solution. This solution was used to prepare the sources for the alpha-spectrometric analysis and for the production of mass-separator targets.

Separation of Pu isotopes was carried out with the electromagnetic mass-separator ISOL-Fasility YASNAPP-2 of LNP [9]. The high temperature ion source with surface ionization was used. The ionizer is a hollow tungsten ampoule (the external diameter is 5 mm, the walls are 1 mm thick, mass is 6 g) heated by the electron bombardment. The ions are extracted through a hole (0.15—0.20 mm in diameter) at the end of the ampoule. The parallel monoenergetic ion beam enters the analysing magnet, where it is mass-separated and focussed vertically and horizontally. the dimensions of the ion beam cross section in the focal plane of the collector chamber are 1 mm vertically and 2 mm horizontally. The cathode power of the ionizer is generally 550—650 W. The mylar foils (11 mm wide and 50 mm long) were used as collectors. The ^{235}U and the ^{238}U isotopes were used as tracers.

Alpha and X-ray spectrometry of the Pu preparation were carried out before and after the mass separation.

Before separation. The aliquots from the Pu fraction obtained from the elution of plutonium by the ion exchange were tested by using a Ge(Li) detector of 80 cm^3 (full width at the half maximum intensity (FWHM) = 3.0 keV at 1.33 MeV) and using a Si(Au) surface barrier detector of 300 mm^2 with the resolution of about 35 keV. The activity of ^{237}Pu has been calculated from the Np – $K_{\alpha 1}$ X-ray peak intensity, the ratios of the activities (Bq/Bq) ^{236}Pu to ^{237}Pu and of ^{238}Pu to ^{237}Pu

were calculated from the alpha peak intensities. The value of a total alpha-branching of $4{,}2 \cdot 10^{-3}$% was used [10]. The sources for the alpha spectrometry were obtained by the electrodeposition.

After separation. The mylar foils after the separation (in analogy with the above described) were analyzed by the X-ray spectrometry to determine the full activity of ^{237}Pu. Then the foils were placed into special shielding cassettes the bottom of which had a 1 mm wide transverse slot. The cassettes were equipped with a device which allowed one to move them above the slot. Inside the cassette the foil length was scanned by Ge(Li) detector at a step of 1 mm between the observable «spots» of separated ^{235}U and ^{238}U. Basing on the results of scanning the location of the ^{237}Pu activity maximum was defined ($\approx$ 2 mm over the foil length) which was cut out. The obtained samples of ^{237}Pu were thoroughly investigated using X-ray, gamma and alpha spectrometry. Low background Ge-detector of (FWHM = 1.2 keV at 122 keV), Ge(Li)-detector of 40 cm^3 (FWHM = 3 keV at 1.33 MeV) and Si(Au) detectors with the resolution of 35 keV (300 mm^2) and 12 keV (7 mm^2) were used.

Results and Discussion

As indicated above the aim of this work is the elaboration of the methods of producing the ^{237}Pu preparation with the ratio ^{236}Pu/^{237}Pu/^{238}Pu = $\leq 10^{-6}/1/\leq 10^{-6}$ (Bq/Bq). Besides, this method is to produce high activity ultra pure ^{237}Pu (at least 100 kBq) to attract practical interest. As was shown in the preliminary experiments, the average efficiency of separating ^{237}Pu from ^{236}Pu and from ^{238}Pu with the YASNAPP-2 mass-separator would be about $8—10 \cdot 10^2$ and $2—4 \cdot 10^2$ correspondingly. The separation yield of ^{237}Pu varied from 20 to 40%.

With the account of the above requirements and the mass-separator possibilities, the conditions of the uranium target irradiation are to ensure the production of the ^{237}Pu preparation with a high yield and with the ratios ^{23}Pu/^{237}Pu and ^{238}Pu/^{237}Pu of about 10^{-4} (Bq/Bq).

Table 1. The results of target irradiation

Target	Energy of ion MeV	^{237}Pu kBq	$^{236}Pu/^{237}Pu$ Bq/Bq	$^{238}Pu/^{237}Pu$ Bq/Bq
U—1	22.0	5.0	10^{-5}	$8.5\cdot10^{-4}$
U—2	22.4	11.0	10^{-5}	$6.0\cdot10^{-4}$
U—3	23.5	9.0	$1.0\cdot10^{-4}$	$2.5\cdot10^{-4}$
U—4	24.0	27.5	$1.6\cdot10^{-4}$	$2.0\cdot10^{-4}$
U—5	24.5	32.5	$2.0\cdot10^{-4}$	$1.5\cdot10^{-4}$
U—6	25.2	37.5	$3.4\cdot10^{-4}$	$1.4\cdot10^{-4}$
U—7	25.8	35.0	$2.5\cdot10^{-4}$	$2.5\cdot10^{-4}$
U—8	26.5	38.0	$7.5\cdot10^{-3}$	$3.0\cdot10^{-4}$

The experimental results given in Table 1 show the activity of ^{237}Pu and the above ratios in the uranium targets. The total charge of the ions for each target was of about $2.0\cdot10^5$ μC.

As can be seen for the 1 $mg\cdot cm^{-2}$ uranium targets the maximum activity of ^{237}Pu was observed at the ^4He-ions energy from 24.0 to 26.5 MeV (targets U4—U8). As was indicated above we used a target block with a cylindrical surface. In this case the calculation of the ^{237}Pu yield per 1 mg of the ^{235}U is difficult since the exact data about the change of the incident angle of the beam to the targets surface are absent.

The targets U1—U8 were irradiated, however, in identical conditions and, thus, the results obtained for the targets U4—U8 indicate that ≈24.0 MeV is the lower end-point energy for producing the high activity ^{237}Pu. The ratios of the activities (Bq/Bq) of the ^{236}Pu and ^{238}Pu to ^{237}Pu, which satisfied the above requirements were observed in the energy range of 23.5—25.2 MeV. With the account of these results, the energy range 24.5—25.0 MeV was chosen for the production of the ^{237}Pu for the mass-separation.

The ^{235}U (99.993%) target 5 $mg\cdot cm^{-2}$ was irradiated with ^4He-ions with the initial energy of 25 MeV at the ion-beam current of about 30 μA during 70 hours. The activity of the ^{237}Pu in the solution after the first anion-exchange column was about 1.5 MBq and the ratio of

Table 2. Energy and relative intensity of α-line ^{237}Pu-preparation

			Count	Intensity (%%) (Stat ERR)		
		^{237}Pu				
1	1.	5654.6	2729	7.8	0.2	18.3 ± 5
	2.	5614.6	2619	7.5	0.2	
	3.	5562.8	1031	2.9	0.1	
	4.	5354.7	2012	5.7	0.2	
	5.	5334.0	15825	45.1	0.6	64.1 ± 1.1
	6.	5300.9	4764	13.6	0.3	
	7.	5256.7	949	2.7	0.1	
	8.	5150.8	3784	10.8	0.2	
	9.	5086.3	287	0.8	0.1	97%
2*	10.	5370.0	260	0.7		
	11.	5220.0	243	0.7		
	12.	5205.0	213	0.6		
	13.	5190.0	136	0.4		
	14.	5173.0	119	0.3		
	15.	5018.0	78	0.2		3%
3		Pu—238 + Pu237?				
		5498.6	328			
		5448.3	67			1.1%
4		Pu—236				
		5767.6	109			
		5718.1	29			0.4%

2* — Estimated value

Pu isotopes was $1.6 \cdot 10^{-4}$ (^{236}Pu/^{237}Pu) and $1.3 \cdot 10^{-4}$ (^{238}Pu/^{237}Pu). After the final anion-exchange column the solution with the activity of 1.2 MBq was obtained.

Two sources with the activity of about 500 kBq each were prepared for the mass-separation. Subsequently two mylar foils were obtained after the separation. The activity of each foil was about 200 kBq, i.e. the separation yield of ^{237}Pu was $\approx 40\%$. The foils were scanned by the X-ray spectrometry as was described in the experimental part and sam-

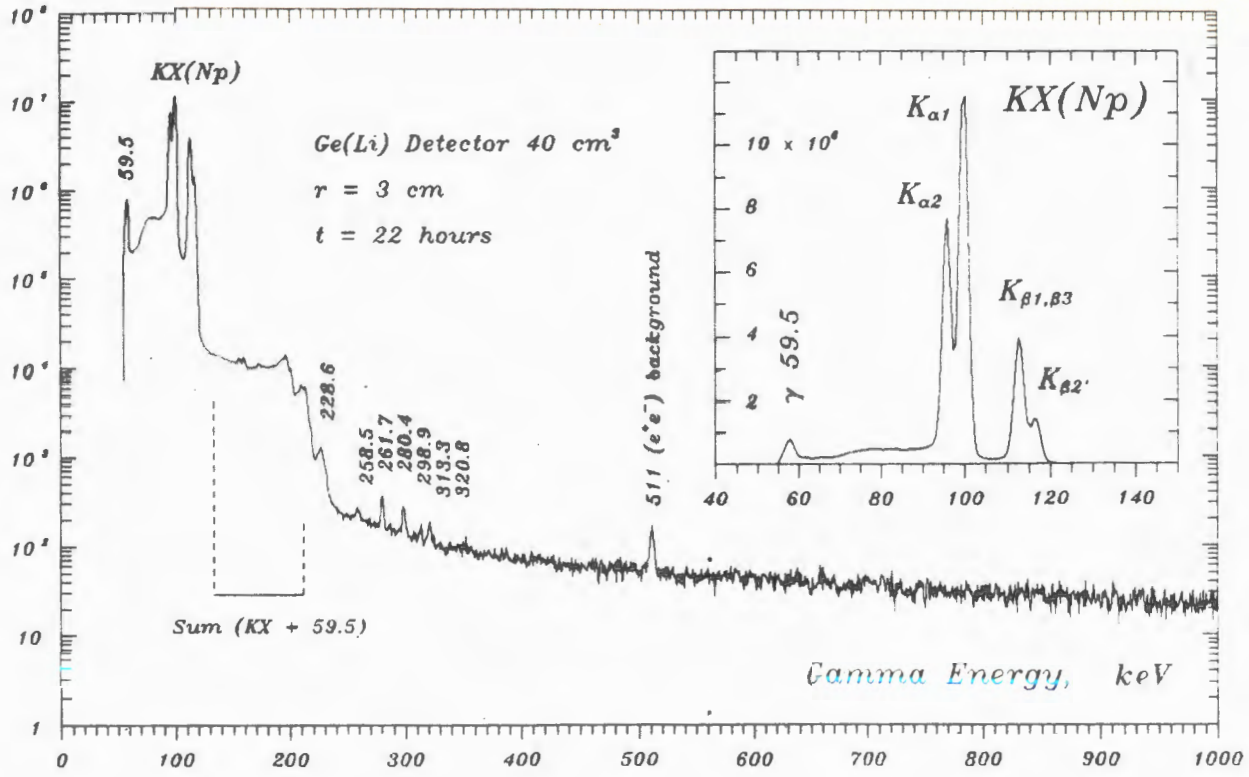
γ-Spectrum of ^{237}Pu
KX(Np)
59.5
Ge(Li) Detector 40 cm³
r = 3 cm
t = 22 hours
228.6
258.5
261.7
280.4
298.9
313.3
320.8
511 (e⁺e⁻) background
Sum (KX + 59.5)
Gamma Energy, keV
KX(Np)
$K_{\alpha 1}$
$K_{\alpha 2}$
$K_{\beta 1,\beta 3}$
$K_{\beta 2'}$
γ 59.5
10 x 10⁴

Fig.1

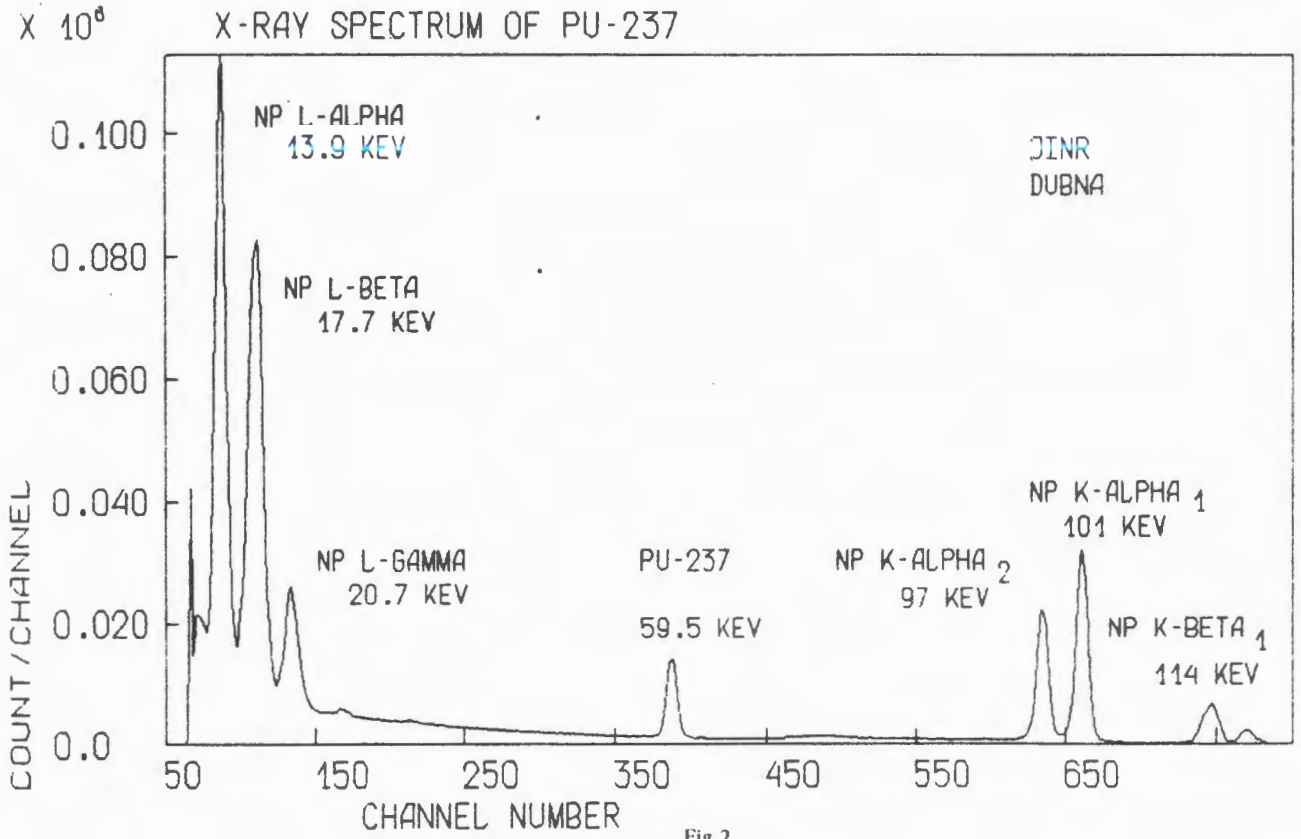
X 10⁶
X-RAY SPECTRUM OF PU-237
NP L-ALPHA
13.9 KEV
NP L-BETA
17.7 KEV
NP L-GAMMA
20.7 KEV
PU-237
59.5 KEV
NP K-ALPHA 2
97 KEV
NP K-ALPHA 1
101 KEV
NP K-BETA 1
114 KEV
JINR
DUBNA
COUNT / CHANNEL
0.100
0.080
0.060
0.040
0.020
0.0
50
150
250
350
450
550
650
CHANNEL NUMBER

Fig.2

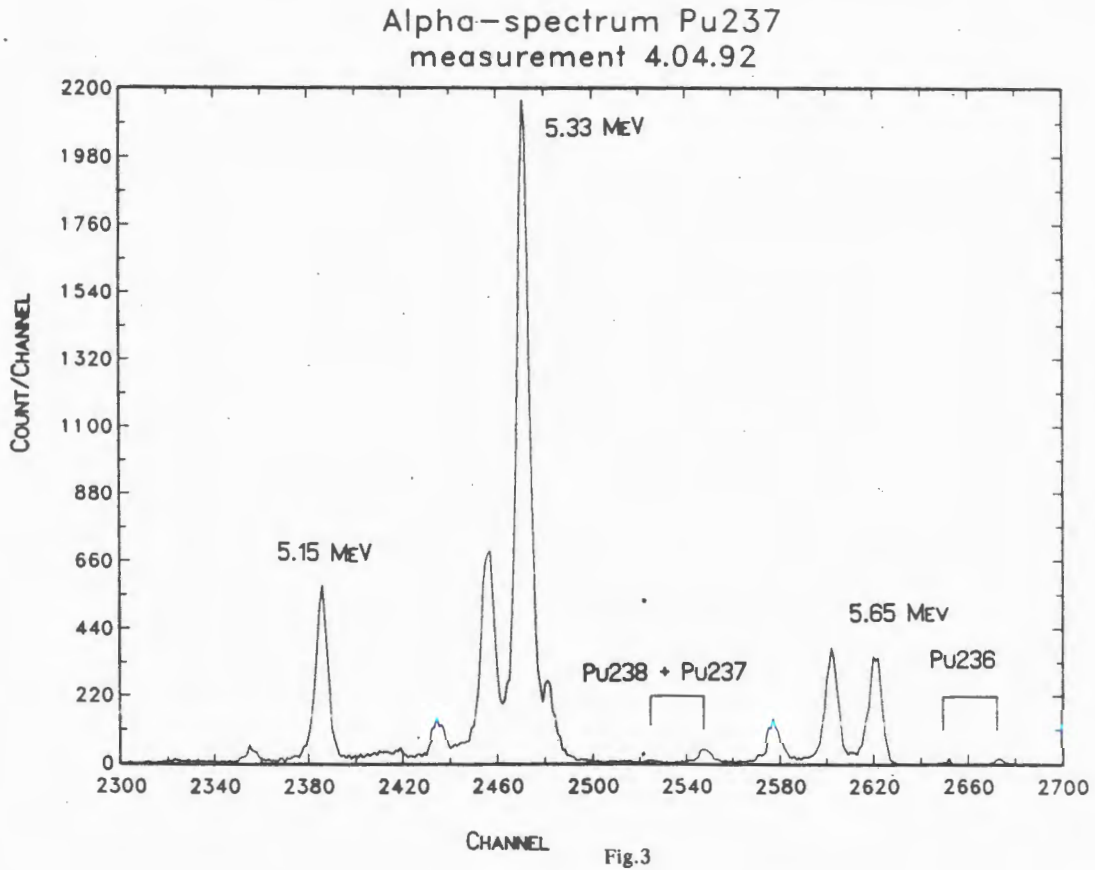
Alpha-spectrum Pu237
measurement 4.04.92
5.33 MeV
5.15 MeV
5.65 MeV
Pu238 + Pu237
Pu236
COUNT/CHANNEL
CHANNEL
2200
1980
1760
1540
1320
1100
880
660
440
220
0
2300
2340
2380
2420
2460
2500
2540
2580
2620
2660
2700

Fig.3

ples of ^{237}Pu (pieces of the foils, 2 mm long) were obtained. The activity of each sample was about 150 kBq. These samples were carefully tested by using Ge, Ge(Li) and Si(Au) detectors. The X-ray and gamma spectrum of ^{237}Pu preparation are given in Figs.1,2. The ratio of Pu isotopes was $2 \cdot 10^{-7}$ ($^{236}Pu/^{237}Pu$) and $3 \cdot 10^{-7}$ ($^{238}Pu/^{237}Pu$).

It should be noted that the determination of the ratios of the plutonium isotope activities was carried out by direct measurements of the alpha-spectra. At using a low background Si(Au) detector of 300 mm^2 with a resolution of 35 keV the measurement time to obtain the statistics necessary for the calculation of isotopic ratio ($\sim n \cdot 10^3$ counts) was from 1 to 4 hr. The analysis of the alpha spectra of the ultra pure ^{237}Pu showed that the number of alpha lines and especially of their relative intensities differ essentially from the data reported before [11]. For more correct determination, the sample of the ultra pure ^{237}Pu with an activity of 140 kBq was tested using a low background Si(Au) detector of 7 mm^2 with a resolution of 12 keV. The resulting spectrum obtained at the 70 hr measurement is given in Fig.3. The value of the energy and the relative intensity normalized over the sum of all the ^{237}Pu alpha lines is given in Table 2. This ^{237}Pu sample was remeasured 45 days later. The absolute intensities of all the alpha line given in Table 2 for the ^{237}Pu were decreased approximately twofold, the relative intensities remained constant.

Conclusion

A techniques for producing radiochemically and isotopically ultra pure ^{237}Pu was developed. The optimal conditions for irradiating the ^{235}U (99,993%) targets at the cyclotron U-200 and for the subsequent separation of the Pu isotopes by the electromagnetic mass-separator YASNAPP-2 were determined.

The ^{237}Pu preparation obtained with $^{236}Pu/^{237}Pu/^{238}Pu$ ratio equal to $2 \cdot 10^{-7}/1/\leq 3 \cdot 10^{-7}$ (Bq/Bq) is the purest one among the preparations reported to date by different Laboratories. The effective dose of this preparations is only 0.0012 mSv/kBq, which is practically equal to that of the monoisotopic ^{237}Pu. The preparation with the above ratio of the alpha-active Pu isotopes is practically harmless for the volunteer's organism at the metabolism study.

This ^{237}Pu preparation (about ~100 kBq) was passed over to the Harwell Biochemical Research Department (Harwell Laboratory, UK) for a metabolism study.

Acknowledgements

Thanks are due to Dr.D.Newton and Dr.E.Voice, who have drawn our attention to the problem of ultra pure ^{237}Pu and who have injected themselves the ^{237}Pu preparation obtained in this work.

References

1. Todt R., Logan R. — J. Appl. Radiat. Isot., 1968, v.19, p.141.
2. Jenkins I.L., Wain A.G. — Int. J. Appl. Radiat. Isot., 1971, v.22, p.429.
3. Ahmad I., Hines J., Gindler J.E. — Phys. Rev., 1983, v.27C, p.2239.
4. Pelevin L.A., Gedeonov A.D., Shuvalov B.I. — Radiochimia, 1988, №6, p.806.
5. Hata K. et al. — Int. J. Appl. Radiat. Isot., 1976, v.27, p.713.
6. Aaltonen J. et al. — Proc. Int. Conf. Actinides-89, Nauka, Moscow, 1989, p.40.
7. Aaltonen J. et al. — Radioanal. Chem., 1981, v.64, p.73.
8. Recommendations of the Int. Com. Radiol. Protect., ICRP Publication 60, Pergamon Press, 1990.
9. Kalinnikov V.G. et al. — JINR, D13-90-183, Dubna, 1990.
10. Ellis Y.A., Emery J.F., Toth K.S. — Phys. Rev., 1979, v.20, p.799.
11. Radionuclide Transformations, ICRP Publication 38, Pergamon Press, p.1159, 1980.

Received on August 25, 1992.

УДК 51-7-73:537

DESIGNING OF THE MAGNETIC SYSTEM BY THE SOLUTION OF INVERSE PROBLEM

E.P.Zhidkov, S.Lima, R.V.Polyakova, I.P.Yudin

In this paper the problem of searching for the design of the magnetic system for creation of a magnetic field with the required characteristics in the given area is solved. On the basis of the analysis of the mathematical model of the magnetic system rather a general approach is proposed to the solving of the inverse problem, which is written by the Fredholm equation:

$$H(z) = \int_S J(s)\, G(z, s)\, ds, \quad z \in U, \quad s \in S,$$

where $J(s)$ is a distributed density function of current in the system, $G(z, s)$ is a Green function, the analytical form of the function depending on the current source geometry and on z point, falling into the definition area of field H. It was necessary to define the current density distribution function $J(s)$ and the existing winding geometry for creation of a required magnetic field. It is known that such problems are incorrect ones. In the paper a method of solving those by means of regularized iterative processes is proposed. On the base of the concrete magnetic system we perform the numerical study of influence of different factors on the character of the magnetic field being designed.

The investigation has been performed at the Laboratory of Computing Techniques and Automation, JINR.

Конструирование магнитной системы при помощи решения обратной задачи магнитостатики

Е.П.Жидков и др.

В данной работе решается задача поиска конструкции магнитной системы для создания магнитного поля с требуемыми характеристиками в заданной области. На основе анализа математической модели магнитной системы предлагается достаточно общий подход к решению нелинейной обратной задачи, которая описывается уравнением Фредгольма:

$$H(z) = \int_S J(s)\, G(z, s)\, ds, \quad z \in U, \quad s \in S,$$

где $J(s)$ — функция распределения плотности тока в системе, $G(z, s)$ — функция Грина, аналитический вид которой зависит от геометрии источников тока и от точки z, принадлежащей области определения поля H. Необходимо определить распределение плотности тока $J(s)$, а также расстановку источников тока для создания поля H. Известно, что такие задачи относятся к классу некорректных задач. В работе предлагается метод решения этих задач с помощью регуляризованных итерационных процессов. На

примере конкретной магнитной системы проводится численное исследование влияния различных факторов на характер создаваемого магнитного поля.

Работа выполнена в Лаборатории вычислительной техники и автоматизации ОИЯИ.

1. Introduction

When designing magnetic system, it is necessary to solve the inverse problem, that is, via a given magnetic field to define current parameters, or its geometrical characteristics, or all that simultaneously.

The definition of the beam density distribution in the magnetic system, in which the geometry is known, is a linear inverse problem for the given field.

When the required field must be created with the help of conductors, in which the value of the curent varies similar to the coordinates of their position, providing the current in all the conductors is the same, we come to the solving of the inverse problem.

In this paper we consider the construction of a mathematical model of the magnetic system for this kind of the problem and the methods and numerical algorithms for their solution by using the Tikhonov regularization methods.

Because a magnetic field is supposed to be given by one of its (H_x, H_y, H_z) components depending on a specific problem, so further H sample will be used for notation.

2. Mathematical Model of the Magnetic System

Let in a region U with the help of the sources of current, distributed in the region S, a field H should be created with the given characteristics (for example, the whole homogeneous field in the region U). It is known [1] that the field in any point z of set U is defined by the expression

$$H(z) = \int_S J(s)\, G(z, s)\, ds, \quad z \in U, \quad s \in S, \tag{1}$$

where $J(s)$ is a distributed density function of the current in the system, $G(z, s)$ is a Green function, that analytically depends both on the geometry of the source of the magnetic system and on the point $z \in U$.

The inverse problem, namely, a definition over the given density of distribution of current in the magnetic system with the known geometry, is a linear inverse problem (model 1).

Then the mathematical problem reduces to the solution of the Fredholm linear integral equation of the first order with unknown function $J(s)$.

If the composition of the magnetic field includes not only variant density of current and arrangement source of current, then we must solve the nonlinear inverse problem (model 2) with unknown $J(s)$ and $s \in S$.

3. Method of Solution of the Inverse Problem (Model 1)

It is known that the problem of solution of the first order Fredholm integral equation (1) is related to the non-correct defined class of the problems, because the large changing in the $J(s)$ solution can correspond to the small changing of the input data $H(z)$. To obtain a stable solution of the non-correct defined problem, A.N.Tikhonov developed a regularized algorithm [2]—[4].

Here we will use the second order method of a regularization in order to solve the problem.

For this, we construct a smooth parametric functional

$$F^{\alpha}\ [J(s), H(z)] = \Phi\ [J(s), H(z)] + \alpha\, \Omega\ [J(s)], \tag{2}$$

where

$$\Phi\ [J(s), H(z)] = \int_U [H(z) - \int_S J(s)\, G(z,s)\, ds]^2\, dz \tag{3}$$

is the quadratic deviation of the operator $A\ [z, J(s)] = \int_S J(s)\, G(z, s)\, ds$ of function $H(z)$, and

$$\Omega\ [J(s)] = \int_S J^2(s) ds \tag{4}$$

is the regularizational functional, or a stable one, and α is a numeric parameter of the regularization ($\alpha > 0$).

Theorem 1. For any function $H(z) \in L_2$ and for any $\alpha > 0$ there exists one and only one $2(n + 1)$ differential function $J_n^{\alpha}(s)$, which realizes the minimum of the smooth functional $F^{\alpha}\ [J(s),\ H(z)]$, of the form (2).

Theorem 2. If $H(z) = A[z, J(s)]$, $J(s) \in C^{(n+1)}$, then for any $\varepsilon > 0$ and auxiliary values $0 < \gamma_1 < \gamma_2$ there exists $\delta(\varepsilon, \gamma_1, \gamma_2, J)$ so that, if

1. $-\| \bar{H}_\delta(z) - {}^*H(z) \|_{L_2} \le \delta$, where $\bar{H}_\delta(z) \in L_2$;

2. $-\alpha = \alpha(\delta)$ has the order δ^2;

3. $-\gamma_1 \le \dfrac{\delta^2}{\alpha(\delta)} \le \gamma^2$,

then $J^\alpha_{\delta, n}(s)$ is a minimum of $F^\alpha_n [J^\alpha_n(s), \bar{H}_\delta(z)]$ and

$\| J^\alpha_{\delta, n}(s)^{(i)} - J^*(s)^{(i)} \| \le \varepsilon$, $s \in S$, $i = 1, 2, ..., n$

with $\delta < \delta_0(\varepsilon, \gamma_1, \gamma_2, J)$.

For this theorem we inference that there exists a function J^α_n, that is a minimum of functional F^α_n in the form (2) which reduces to the solution of the equation (1) $J(s)$. The complete demonstration of this and other conditions one finds in [4].

When applying the regularization method, the selection of parameter α is one of the main problems.

The point is that not always for the obtained smooth solution the discrepancy principle is being fulfilled, i.e. there exists the inequality

$$\| \bar{H}_\delta - H^* \| \le \delta, \tag{5}$$

where δ is precision of the approximate input data $\bar{H}_\delta$, H^* is the precise value of the input data.

In practice, for the solution of the non-correct problem it is necessary to find the solution, that satisfies the required precision. In [5] V.A.Morozov suggested, as the main quality criteria, to select the regularization parameter of the deflection principle.

Discrepancy Principle. Set any $0 < \delta \le \delta_0$ and any $0 < h \le h_0$ with condition

$$\chi(h, \delta, J) = (\| A_h J - AJ \|_0 + \delta) \times (1 + \beta(\delta, h))^{1/2} < \| A_h J - \bar{H}_\delta \|_0,$$

where $\beta(\delta, h)$ is a positive function, such that $\lim_{\delta, h \to 0} \beta(\delta, h) = 0$, and J^α is the solution obtained for the minimum of functional $F^\alpha(J, H)$.

Then there exists at least one value of the regularization parameter $\alpha = \alpha(\delta, h) > 0$, so that

$$\rho_{\delta h}(\alpha(\delta, h)) = \chi^2(h, \delta, J),$$

and

$$\lim_{\delta, h \to 0} J^{\alpha}_{\delta h} = J^{\alpha} \quad \text{and} \quad J^{\alpha}_{\delta h} = J^{\alpha(\delta, h)}_{\delta h}.$$

4. Numerical Algorithm for the Solution of the Problem of Model 1

In the expression (2), if presenting the integral in the form of sums, we obtain

$$F^{\alpha} = \sum_{j=1}^{N} \left[H_j(z_j) - \sum_{i=1}^{M} J_i(s_i) K_{ij}(z_j, s_i) \right]^2 \Delta z_j + \alpha \sum_{i=1}^{M} J_i^2(s_i) \Delta s_i, \tag{6}$$

where N is a number of points from the set U, M is a number of points from the set S, $M \leq N$ and $K_{ij} = \int_{\Delta s_i} G(z_j, s)\, ds$.

Suppose $\Delta s_i = \Delta s = \text{const}$, $\Delta z_j = \Delta z = \text{const}$.

The condition of the minimum of the functional F^{α} is

$$\frac{\partial F^{\alpha}}{\partial J_1} = 0, \quad \frac{\partial F^{\alpha}}{\partial J_2} = 0, \ldots, \quad \frac{\partial F^{\alpha}}{\partial J_M} = 0. \tag{7}$$

Taking into account (6), we obtain

$$\frac{\partial F^{\alpha}}{\partial J_l} = -\sum_{j=1}^{N} H_j K_{lj} \Delta z + \sum_{j=1}^{N} \sum_{i=1}^{M} J_i K_{lj} K_{ij} \Delta z + \alpha J_l \Delta_s = 0,$$

$$l = 1 \div M. \tag{8}$$

In such a way we have a system M linear algebraic equations with the unknowns N of the J_l form:

$$\sum_{i=1}^{M} J_i \sum_{j=1}^{N} K_{lj} K_{ij} \Delta z + \alpha J_l \Delta s = \sum_{j=1}^{N} H_j K_{lj} \Delta z, \quad l = 1 \div M. \tag{9}$$

Supposing $\alpha \Delta s = \alpha' \Delta z$, we obtain

$$\sum_{i=1}^{M} J_i \sum_{j=1}^{N} K_{lj} K_{ij} + \alpha' J_l \Delta s = \sum_{j=1}^{N} H_j K_{lj}, \quad l = 1 \div M. \tag{10}$$

Obviously, α' serves the meaning of arbitrary coefficient α, therefore the system of equations for J_1 we can write finally definitively in the form

$$\sum_{i=1}^{M} J_i \sum_{j=1}^{N} K_{lj} K_{ij} + \alpha J_l = \sum_{j=1}^{N} H_j K_{lj}, \quad l = 1 \div M. \tag{11}$$

If the magnetic system is a discrete set of coils, then the field $H(z)$ in any point $z \in U$ is defined in the following way:

$$H(z) = \sum_{i=1}^{M} J_i \int_{\Delta s_i} G(z, s)\, ds, \tag{12}$$

where M is a number of coils, J_i is the current density in the i-th coil, Δs_i is the selection of the i-th coil.

Having solved the system of equations (11), we obtain a discrete set J_l, $l = 1 \div M$, that is a solution of the problem (1). Similar to that, we define the distribution of the current density in the magnetic system for creation of field $H(z_j)$, $j = 1 \div N$, $z_j \in U$.

5. Particular Case of the Mathematical Model 2

Let in some region S with a disposition M of conductors with the same current I_0, the field H be created.

In the system $H(z)$, $z \in U$ we have

$$H(z) = I_0 \sum_{i=1}^{M} G(s_i, z), \tag{13}$$

where $G(s_i, z)$ is the Green function for the i-th conductor.

Both a current I_0 and the coordinates s_i of the conductors, which would provide the given field $H(z)$, $z \in U$ in a best way, should be defined.

The function $G(s_i, z)$ is usually a nonlinear one concerning the coordinate of the conductors s_i, therefore the analysed problem is a nonlinear inverse problem.

Additional difficulty in the solving of the inverse problem is the restriction in the parameters [6]. However in any particular case one can

efficiently find a solution for the given condition of the problem. Let us consider this case.

Let a parameter of the conductors disposition in the region S be only one coordinate, for example x, the region of disposition of the conductors in the axis x being known, $x_1 \leq x_i \leq x_2$.

Then the equation (13) will have the form:

$$H(z) = I_0 \sum_{i=1}^{M} G(x_i, z), \quad z \in U, \quad x_1 \leq x_i \leq X_2. \tag{14}$$

We must define I_0, x_i to create the field $H(z)$, $z \in U$, in the magnetic system. The problem (14) is a non-linear inverse problem.

6. Numeric Algorithm of the Solution of the Problem in Model 2

The solution of the problem (14) was divided into two steps. In the first step, the current density in the twisters is continuously distributed in the range of the given problem. The equation (13) has the form

$$H(z) = \int_{x_1}^{x_2} J(x)\, G(x, z)\, dx.$$

This problem and the algorithm of its solution was analysed in the points 2, 3. To select the solution $J^{\alpha}(x)$, (α is the regularization parameter) we calculate the following conditions of the problem:

1. The precision of the calculation of $H(z)$ cannot be worse than the required precision of the magnetic field in the created magnetic system;

2. For all permissible interval $[x_1, x_2]$, a function $J^{\alpha}(x)$ must keep the sign;

3. $|J^{\alpha}(x)| \leq J_{dop}$ is the permissible current density.

Suppose, that there exists a continuous solution $J^{\alpha}(x)$, that satisfies all three conditions.

In the second step, we divide the interval $[x_1, x_2]$ in M subintervals $[x_1^i, x_2^i]$, $i = 1 \div M$.

Then

$$H(z) = \sum_{i=1}^{M} \int_{x_1^i}^{x_2^i} J^{\alpha}(x)\, G(x, z)\, dx, \quad z \in U. \tag{15}$$

For each subinterval $[x_1^i, x_2^i]$, the conditions of the theorems about the mean value (as function $J^\alpha(x)$ was chosen) are satisfied, therefore

$$H(z_j) = \sum_{i=1}^{M} G(x_i^j, z_j) \int_{x_1^i}^{x_2^i} J^\alpha(x)dx, \quad J = 1 + N, \tag{16}$$

where N is a number of points in the region U, in which field H is analysed, x_i^j is a point in the i-th intervals. The limits x_1^i, x_2^i, were chosen in order to

$$\int_{x_1^i}^{x_2^i} J^\alpha(x)dx = \int_{x_1^{i+1}}^{x_2^{i+1}} J^\alpha(x)dx = I_0, \text{ i.e.,}$$

$$I_0 = \frac{\int_{x_1}^{x_2} J^\alpha(x)dx}{M}, \tag{17}$$

then

$$H(z_j) = I_0 \sum_{i=1}^{M} G(x_i^j, z_j). \tag{18}$$

Obviously, for different z_j there exists its point x_i^j, but based on the theorem of the mean values it always is in the intervals $[x_1^i, x_2^i]$. This means that unknown coordinate x_i is too in the i-th interval and it is defined from the condition of minimum of the functional

$$\varphi(x_i) = \sum_{j=1}^{N} \left[\int_{x_1^i}^{x_2^i} J^\alpha(x)\, G(x, z_j)\, dx - I_0 G(x_i, z_j) \right]^2 \tag{19}$$

$$\frac{\partial \varphi(x_i)}{\partial x_i} = \sum_{j=1}^{N} \left[\int_{x_1^i}^{x_2^i} J^\alpha(x)\, G(x, z_j)\, dx - I_0 G(x_i, z_j) \right] \times$$

$$\times \frac{\partial G(x_i, z_j)}{\partial x_i} = 0.$$

$$x_1^i \le x_i \le x_2^i \tag{20}$$

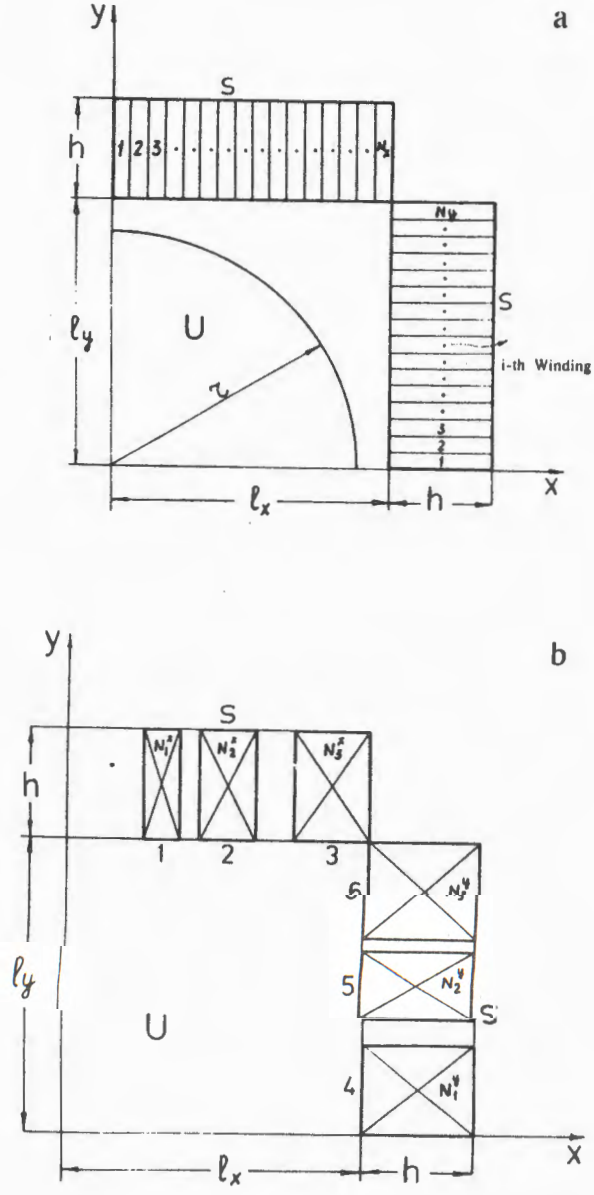

Fig.1 a, b. The bipolar SP configuration in the plane of the winding; b — one of the possible real SP configurations

Then the solution of the problem is reduced to the solving of M sequential nonlinear equations in the form (20) with one unknown, moreover, the limits of the existence of the solution are known.

Note that we have analyzed the algorithms for creating a magnetic system with infinite thin conductor.

It's easy to demonstrate that for the finite size of the conductor the algorithms completely keep, only in this case the Green function goes under the sign of integration by the section of the conductor.

When the permissible geometrical region of arranging the conductor defines as the nonlinear one, the density does not involve particular difficulties, too, and can be described by the similar algorithm.

7. Example of a Numerical Calculation of Real Magnetic System

Let us see an example of practically developed application of the algorithm to create non-metallic superconductor (SP) of the bipolar magnet, that was composed by triangular winding of excitement (its geometry is shown in Fig.1).

From Fig.1 it is obvious that the magnetic system was composed by triangular winding and it has a perimeter dimension of the aperture of magnet.

Using the developed numerical algorithm for the nonlinear inverse solution we calculate the mathematical model of the system, with a homogeneous field in which 80% of the aperture represent $10^{-5} + 10^{-6}$ for the magnitude of file 4—5.

The mathematical problem was set in the following mode.

Let in some region (see Fig.1a) an homogeneous field $H(z)$, $z \in U$ be created, using an arrangement M of the conductors of the triangular section in the given limited region S with condition that the current I_0 for all conductors is the same. For this magnetic system

$$H(z) = I_0 \sum_{i=1}^{M} G(s_i, z), \quad s_i \in S, \quad z \in U. \tag{21}$$

In Descartes system of coordinates $s_i = \{x_i, y_i\}$, $z = \{x, y\}$

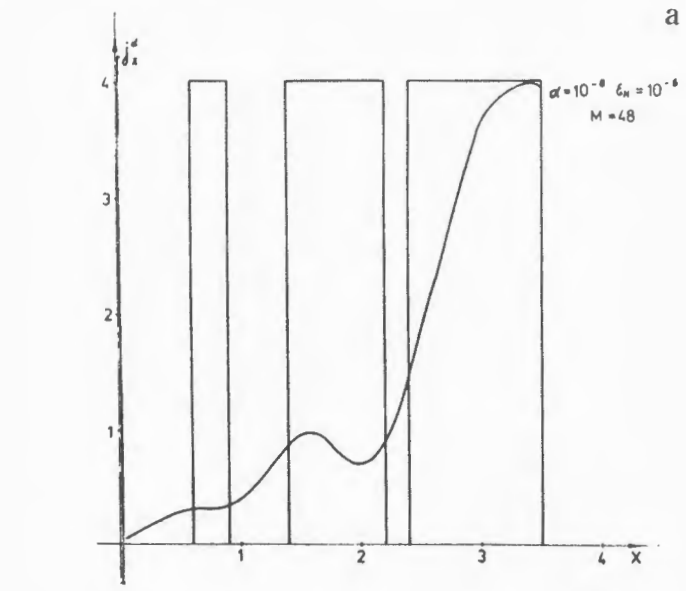

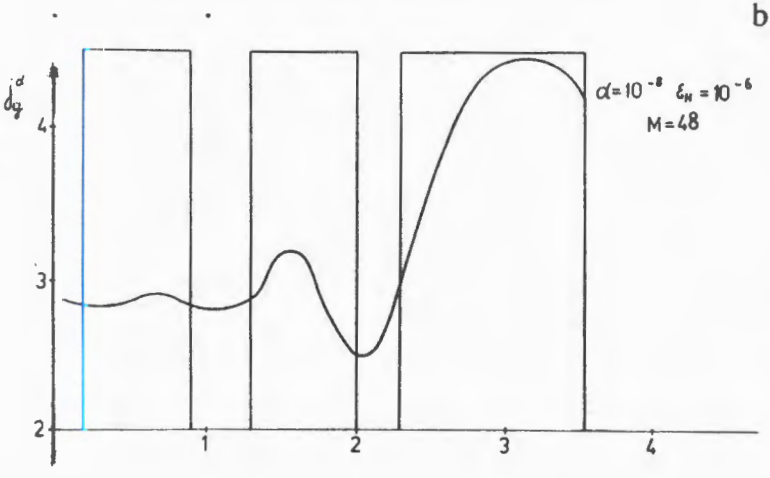

Fig.2 a, b. The continuous distribution $J^{\alpha}(s)$ and the approximation $J^{\alpha}(s)$ of the constant subinterval function «blocks»

$$G(s_i, z) = \frac{y - y_i + b}{2} \ln \frac{(x - x_i + a)^2 + (y - y_i + b)^2}{(x - x_i - a)^2 + (y - y_i + b)^2} + \tag{22}$$

$$+ \frac{y - y_i - b}{2} \ln \frac{(x - x_i - a)^2 + (y - y_i - b)^2}{(x - x_i + a)^2 + (y - y_i - b)^2} +$$

$$+ (x - x_i + a) \times \left\{ \operatorname{arctg} \frac{x - x_i + a}{y - y_i - b} - \operatorname{arctg} \frac{x - x_i + a}{y - y_i + b} \right\} +$$

$$+ (x - x_i - a) \times \left\{ \operatorname{arctg} \frac{x - x_i - a}{y - y_i + b} - \operatorname{arctg} \frac{x - x_i - a}{y - y_i - b} \right\},$$

where a is the half-dimension of the tire along x, is the half-dimension of the tire along y, is the Green function for the triangular tire in the Descartes system of coordinates [1].

$$= N_x + N_y,$$

N_x is the number of the creep tire of axis x, N_y is the number of the creep tire of axis y, or

$$M = \sum_{i=1}^{k} N_l,$$

k is the number of the winding blocks, and N_l is the number of the creeps in the 1-th blocks.

We must define not only I_0, but undetermine the block configuration that forms the homogeneous field $H(z)$ for every point $z \in U$ with a precision non less $10^{-5} - 10^{-6}$.

In Fig.2 continuous distribution J_x^{α} and J_y^{α} for $M = 48$ creep and the approximation of its continuous «blocks» function for each subinterval are given.

The Table contains the numerical calculation for the optimal variant of the magnet, an in Fig.1b the scheme of this magnet is presented.

8. Conclusion

1. In this paper we analyze the method of solving the nonlinear inverse problems which are necessary for the description of the mathematical model of magnetic system of some class.

Table. Values of the coordinate of this «blocks» center for x and y, given by the best related precision of lower harmonics in the homogenous field H

		x = cosnt = 3.8					y = const = 3.8			
N_y	N_{k1} . . . N_2 N_1	y_1	y_2	y_3	N_x	N_{k2} . . . N_2 N_1	x_1	x_2	x_3	Averaged related precision of the lower harmonics c_2, c_4, c_6
20	10 5 5	0.509	1.5972	2.8588	9	6 2 1	1.0017	2.2937	3.1406	$0.3\times10^{-6}\div0.5\times10^{-6}$
20	12 8	0.8421	2.6494		9	6 2 1	1.6024	2.2468	3.225	$0.9\times10^{-5}\div0.45\times10^{-6}$

2. The developed numerical algorithm, based on the method of regularization of the solution of non-correct problems with restrictions in the searched parameters, is reduced to the nonlinear type of problem (14) for the solution of M sequential nonlinear equations with one incognita. It permits one to avoid difficulties, related to the solution of the system of the nonlinear equations. This solution is frequently reduced to the inverse problem.

3. To realize the proposed method in a computer a numerical algorithm was developed and a Fortran programs package was written.

4. Using this complex program, some practical problems [7], [8] were solved, one of those was analyzed as an example in section 7.

5. The results of the numerical modeling of some real system were used for designing and creating the supperconducting accelerator of High Energy Laboratory, JINR.

9. References

1. Brekhna H. — Supperconducting Magnetic Systems, Moscow, «Mir», 1976.
2. Tikhonov A.N. — DAN, 1963, V.153, N1, p.49—52.
3. Tikhonov A.N. — DAN, 1963, V.151, N3, p.501—504.
4. Arsenin V.Ya., Tikhonov A.N. — Method of the Solution of Non-Correct Problem. Moscow, «Nauka», 1979.
5. Morozov V.A. — Numerical Methods and Programming. Issue, 8, Publication MSU, 1967, pp.63—25.
6. Polyak B.T. — Iteration Methods of Solution of Any Non-Correct Variation Problems. Numerical Methods and Programming. Issue 12, Publication MSU, 1969, 38—52.
7. Zhidkov E.P., Polyakova R.V., Shelaev I.A., Zynovjeva — Solution of the Any Nonlinear Magnetostatic Class Inverse Problem. JINR, 11-10845, Dubna, 1977.
8. Zhidkov E.P., Polyakova R.V., Kuts V., Shelaev I.A., Yudin I.P. — Solution of Some Nonlinear Magnetostatic Inverse Problem. JINR, 11-88-335, Dubna, 1988.

Received on August 28, 1992.

УДК 539.12....162.3

NEW EFFECTIVE MASS IN ADIABATIC APPROACH FOR THE MUONIC THREE-BODY PROBLEM

I.V.Puzynin, T.P.Puzynina, Yu.S.Smirnov, S.I.Vinitsky

The method for the construction of the adiabatic equation describing the discrete and continuous spectra of the mesic molecule systems by means of the generalization of the concept of the effective mass is presented.

The investigation has been performed at the Laboratory of Computing Techniques and Automation, JINR.

Новая эффективная масса в адиабатическом подходе для мюонной задачи трех тел

И.В.Пузынин, Т.П.Пузынина, Ю.С.Смирнов, С.И.Виницкий

Предложен метод построения адиабатического уравнения для описания дискретного и непрерывного спектров мезомолекулярных систем путем обобщения понятия эффективной массы.

Работа выполнена в Лаборатории вычислительной техники и автоматизации ОИЯИ.

In this work we discuss our numerical experiments on calculating the energy levels of mesic molecules and mesic atoms cross sections in the framework of some adiabatic approaches. The performed analysis, first, has to explain the known disagreements between adiabatic and variational calculations of the energy levels of the weakly bound states of $dd\mu$ and $dt\mu$ molecules and, second, to give the basis for the construction of new effective adiabatic equations describing adequately both discrete and continuous spectra of mesic molecular systems. We called the above disagreement «the white hole» in the history of μcF theory [1]. Let us remember this disagreement. In 1984 we obtained the following values of the weakly bound states energy in the three-body adiabatic representation

$-\varepsilon_{11}\ (dd\mu)$	$-\varepsilon_{11}\ (dt\mu)$
1.956 ± 0.001 (eV)	0.656 ± 0.001 (eV).

We used 884 states of the two centers problem, in particular , 52 states of the discrete spectrum and 832 states of the continuous one. Our adiabatic results have stimulated the direct variational calculations [2]. However later in our variational calculations we obtained the more accurate values

$-\varepsilon_{11}\,(dd\mu)$	$-\varepsilon_{11}\,(dt\mu)$
1.97475 (eV)	0.6600 (eV).

In these calculations [3] we used about 2660 variational functions. Since up to now we have «a monopoly» in adiabatic calculations of the binding states of mesic molecules, we suggest the explanation of the disagreements mentioned above. We think that this will be useful for the correct applications of adiabatic approaches in the muonic three-body scattering problem and other problems.

The adiabatic representation [4] is based on the expansion of the Shroedinger three-body wave function $\Psi(\overline{R}, \overline{r})$ over a complete set of two center problem solutions

$$\Psi(\overline{R}, \overline{r}) = \sum_j \Phi_j(\overline{r}, \overline{R})\, R^{-1}\chi_j(R). \qquad (1)$$

Using formally the Kantorovich method for reducing a partial differential equation to a set of ordinary ones we obtain the infinite system of radial equations

$$\left[\frac{d^2}{dR^2} + 2ME - U_{ii}(R)\right]\chi_i(R) = \sum_{i \neq j} U_{ij}(R)\chi_j(R). \qquad (2)$$

Here

$$U^J_{ii}(R) = 2ME_i(R) + \frac{1}{R} + H^{AD}_{ii}(R) + \frac{J(J+1) - 2m^2}{R^2},$$

$$H^{AD}_{ii}(R) = \langle \frac{\partial}{\partial R}\Phi_i | \frac{\partial}{\partial R}\Phi_i \rangle,$$

$$U^J_{ij} = H_{ij}(R) + \frac{d}{dR}Q_{ij}(R) + 2Q_{ij}\frac{d}{dR} + B^J_{ij}(R).$$

We have proposed the boundary conditions of radial wave functions for bound states and the scattering problem, which allows the same treatment for both problems as a nonlinear functional equation. For solving this equation we have constructed a new numerical method [2], that is a generalization of the continuous Newton method.

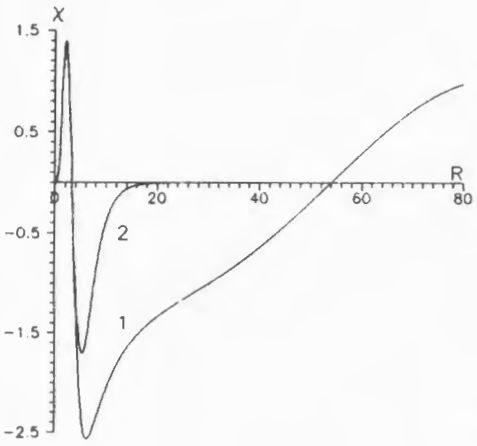

Fig. 1. The radial wave functions 1 — $\chi_1^{(1)}$ for the open and 2 — $\chi_2^{(1)}$ for the closed channels in the reaction of the resonant scattering $(t\mu)_{n=1} + d \to (t\mu)_{n=1} + d$ with orbital momentum $J = 1$

Our first adiabatic calculations were performed in the two level approximation. In 1975 first we obtained the quasy-stationary state of the $dt\mu$ molecule with the total orbital momentum $J = 1$ and $M = 10.894$ (in this units of reduced mass $m^* = 202.024 m_e$). For this mass we found the energy

$$-\varepsilon = E = 0.68 \text{ eV} \quad (E \equiv \widetilde{E} - E_1(\infty))$$

and the width

$$\Gamma = 10.87 \text{ eV}.$$

The radial wave functions $\chi_1^{(1)}(R)$ for the open channel and $\chi_2^{(1)}(R)$ for the closed channel in the case of the elastic scattering

$$(t\mu)_{1s} + d \to (t\mu)_{1s} + d$$

are displayed in fig.1.

This result however was not published in ref.[5]. Now we have reproduced the transformation of this state to the weakly bound state when the

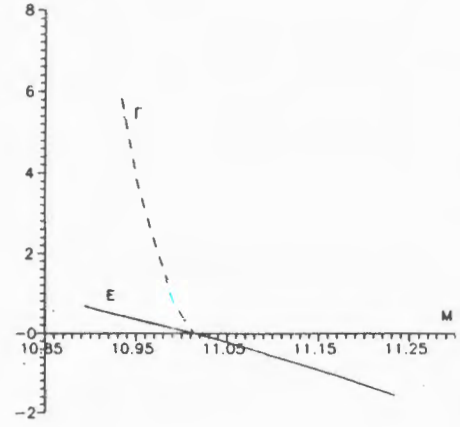

Fig. 2. The dependence of the energy E (eV) and width Γ (eV) of the $dt\mu$ -mesic molecule ($J = 1$, $v = 1$) on the ellective mass M

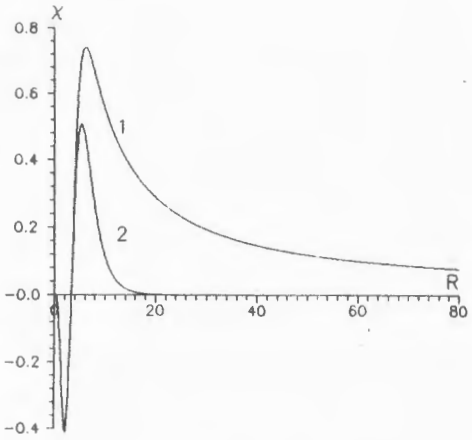

Fig. 3. The radial wave functions 1 — $\chi_1^{(1)}$ and 2 — $\chi_2^{(1)}$ for the $J = 1$ and the zero collision energy $\varepsilon = 0$ $,(t\mu)_{n=1} + d \to (t\mu)_{n=1} + d$

effective mass M increases as parameter.

Figure 2 shows the dependence of the energy E and the width Γ on such a mass. For the mass value $M \approx 11.01$ we have the state with the zero energy and the zero width. The radial functions of such case are presented in fig.3. The function 1 of the open channel is decreasing slowly in comparison with the function 2 of the closed channel. As the mass M increases, the $dt\mu$ system is transferred to the bound state. For the value $M \approx 11.12$ eV we have obtained the «symmetrical» value of the energy $E = -0.68$ eV. Therefore we can expect that the weakly bound state ($J = 1$, $v = 1$) exists and the value of the binding energy is similar to this one if we take into account all the non-adiabatic corrections to the energy level. Indeed, our adiabatic and variational results are near to this value. We have the function $E = E(M)$ and we can find for the «exact» value $E = -0.66$ eV the corresponding value of the effective mass $M \approx 11.11$. The radial functions of this state are presented in fig.4.

Thus we have reproduced the variational energy level by choosing the effective mass M in the two level adiabatic approximation.

We have performed the calculations of the cross-section of the reaction

$$(t\mu)_{1s} + d \to (t\mu)_{1s} + d$$

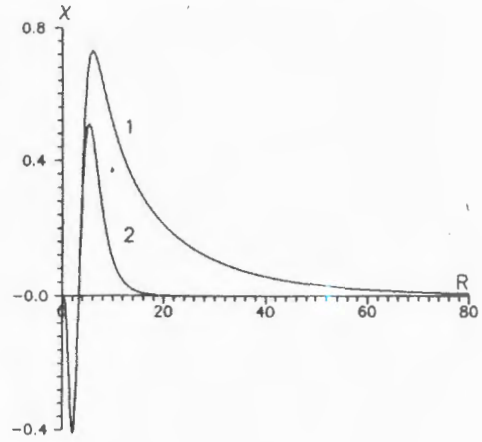

Fig. 4. The radial wave functions 1 — $\chi_1^{(1)}$ and 2 — $\chi_2^{(1)}$ of the bound state ($J = 1$, $v = 1$) of the $dt\mu$-mesic molecule

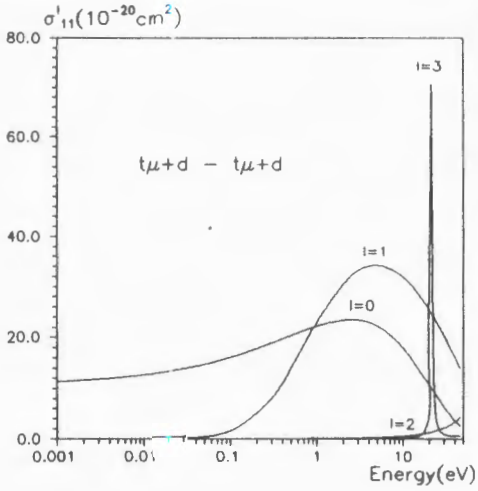

Fig. 5. Partial eleastic scattering cross sections of $t\mu$-atoms on deuterium nuclei

using corresponding value of M. Our results of calculating partial (σ^l_{11}) and total (σ_{11}) elastic scattering cross sections of $t\mu$ - atoms on deuterium nuclei d (see figs.5,6) agree with other multichannel calculations [6] and reproduce the known form resonance for $J = 3$ and $E \approx 21$ eV. The radial wave functions $\chi_1^{(1)}$, $\chi_2^{(1)}$ and $\chi_1^{(2)}$, $\chi_2^{(2)}$ corresponding to the reactions

$$(t\mu)_1 s + d \to (t\mu)_{1s} + d$$

and

$$(d\mu)_{1s} + t \to d + (t\mu)_{1s}$$

are presented in figs.7—8.

A natural generalization of effective mass as a variable parameter appeared in the new effective two level approximation when we take into account non-adiabatic corrections truly. We have obtained them by means of a canonical operator transformation $T = T(R, d/dR)$. This transformation excludes nondiagonal terms in the right-hand side of the equation (2), including the operator terms $2Q(R)\, d/dR$. Thus, the above transformation

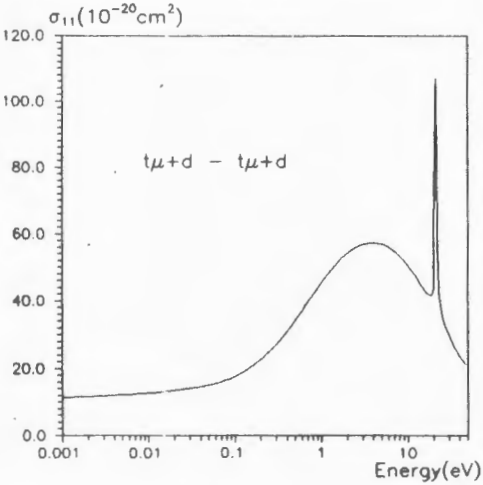

Fig. 6. Total eleastic scattering cross sections of $t\mu$-atoms on deuterium nuclei

Fig. 7. The radial wave functions 1 — $\psi_1^{(1)}$ and 2 — $\psi_2^{(1)}$ for the $l = 0$ corresponding to the scattering process $(t\mu) + d$ with two open channels at the collision energy $E = 0.3$ eV (above the second threshold)

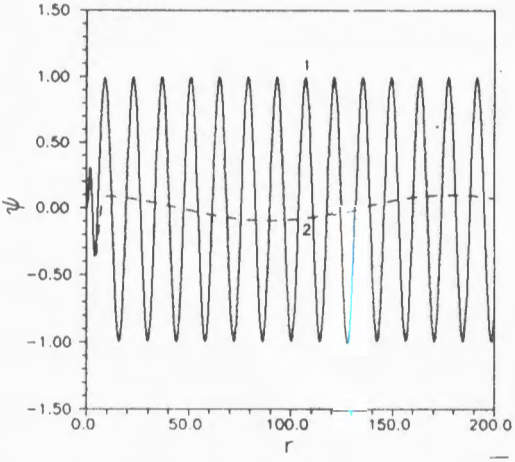

Fig. 8. The radial wave functions 1 — $\psi_1^{(2)}$ and 2 — $\psi_2^{(2)}$ for the $l = 0$ corresponding to the scattering process $(d\mu) + t$ with two open channels at the same collision energy $E = 0.3$ eV

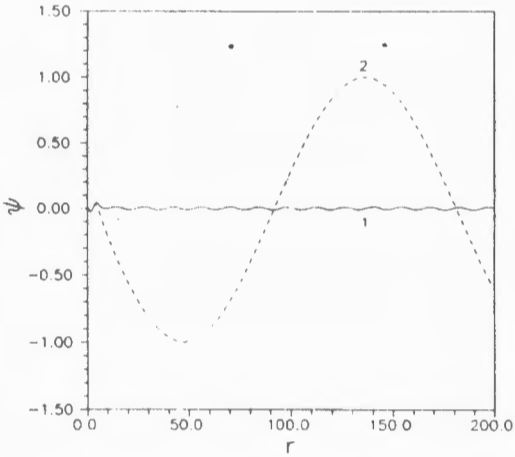

is the generalization of the known Best Adiabatic Approximation [7]. Finally we have obtained the new system of equations

$$\{\delta M\mu^{-1}(R)\frac{d^2}{dR^2} - \delta M[2\tilde{Q}(R, M)\frac{d}{dR} + \tilde{V}(R, M)] + \tilde{p}^2\}\chi(R, \tilde{p}) = 0. \quad (3)$$

Here $\tilde{p} = 2M\varepsilon$ is the matrix of channel momenta,

$$\tilde{Q}(R, M) = Q(R) + (2M)^{-1}\Delta Q(R),$$

$$\tilde{V}(R, M) = V(R, M) + (2M)^{-1}\Delta V(R)$$

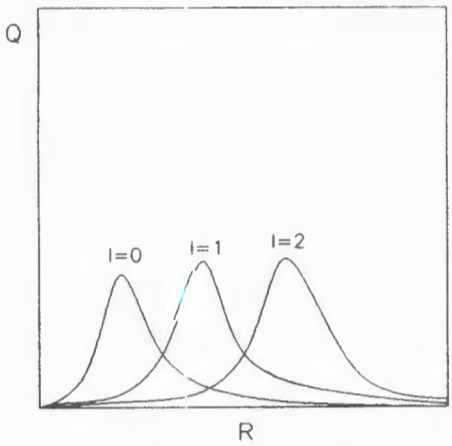

Fig. 9. The behaviour of the matrix elements $Q(R)$ relating to continuous spectrum

are the new potentials;

$$\mu^{-1}(R) = 1 + (2M)^{-1}\Delta\mu^{-1}(R)$$

is the new effective mass depending on R and satisfying the asymptotic condition

$$\delta M\mu^{-1}(R) \to 1 \qquad (4)$$

if $R \to \infty$. Note, that $\delta M = \mathbf{M}/M$ is the matrix of corrections between the Jacobi $\mathbf{M}$ and the adiabatic M masses;

$$-\Delta\mu_{ii}^{-1}(R) = 4\sum_{j\neq i}^{\infty} Q_{ij}(R)Q_{ji}(R)(E_i(R) - E_j(R))^{-1} \qquad (5)$$

are diagonal corrections to unit. The relation (5) is valid only if the sum is complete. Since in the calculations this sum has a finite number of terms, the relation (4) is not valid exactly.

On the other hand we have the approximate relation

$$\mu^{-1}(\infty) = 1 - (2M)^{-1}\frac{1}{2} \approx 0.973 \qquad (6)$$

$$(2M)^{-1} \approx 0.05339 \text{ (exactly for } dd\mu).$$

If we use only the finite number of states of the continuous spectrum, then we have the following value

$$\tilde{\mu}^{-1}(\infty) = 1 - (2M)^{-1}0.28 = 0.985. \qquad (7)$$

We explain this fact by the specific behaviour of the matrix elements relating to the continuous spectrum. This behaviour is schematically shown in fig.9.

Therefore if l is fixed and $R \to \infty$, the contribution of the continuous spectrum is lost in formula (6) since it is a locally incomplete set.

As a result we have

$$|(\mu^{-1}(\infty) - \tilde{\mu}^{-1}(\infty))/\mu^{-1}(\infty)| \approx 1\%.$$

Fig. 10. The cross section σ_{11}^{0} $(10^{-19}$ cm$^2)$ for reaction $p\mu\ (F = 0) + p \to p\mu\ (F' = 0) + p$, s = 1/2

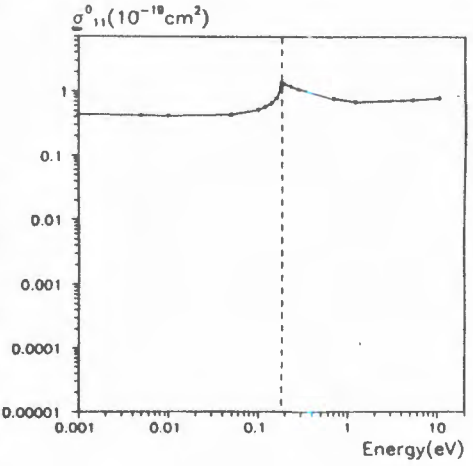

The relative difference between variational and adiabatic results is also about 1% for both $dd\mu$ and $dt\mu$ weakly bound states.

The simplest variant of the proposed approach consists in using the relation (4) on whole interval $0 \le R < \infty$.

Then we obtain a two level approximation

$$\{\frac{d^2}{dR^2} - \delta M\ [2Q(R)\ \frac{d}{dR} + V(R, M)\ ] + \tilde{p}^2\}\ \chi(R, \tilde{p}) + 0, \tag{8}$$

where δM is a variable parameter.

Note that we can find this parameter with a fit of the discrete spectrum and then use the equation (8) for the calculation of the cross sections of mesic atoms.

We have considered the more complicated case for using the new effective mass. We have calculated the cross section of the scattering process

$$p\mu\ (\uparrow\downarrow) + p \to p\mu\ \ (\uparrow\downarrow) + p$$

and obtained the true treshold behaviour as on fig.10. For this example in fig.11, 12 we demonstrate also the corresponding behaviour of the new effective mass and the potential from the eq.(3).

We intend now to solve the inverse spectral problem in two-level adiabatic approximation

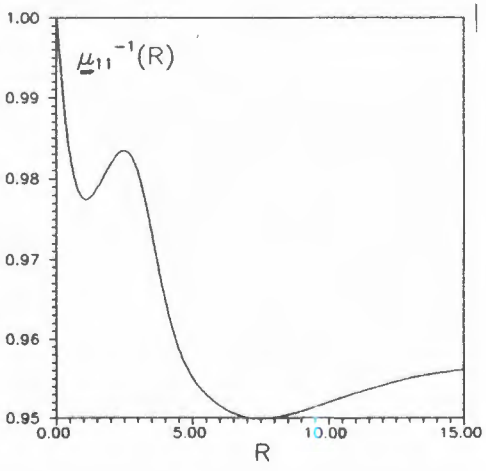

Fig. 11. The effective mass μ^{-1} (R) of the mesic molecul $pp\mu$ for $J = 0$

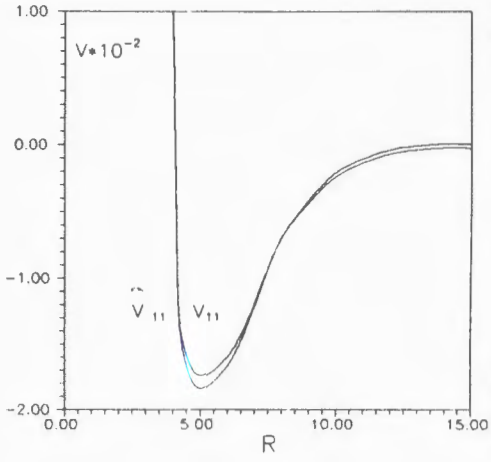

Fig. 12. The effective $\tilde{V}$ and adiabatic V potentials of the mesic molecule $pp\mu$, $J = 0$

for the investigation of the new effective masses of muonic systems.

References

1. Ponomarev L.I., Fiorentini G. — Muon Catalysed Fusion, 1987, 1, p.3.
2. Puzynin I.V., Vinitsky S.I. — Muon Catalysed Fusion, 1988, 3, p.307.
3. Korobov V.I., Puzynin I.V., Vinitsky S.I. — Muon Catalysed Fusion, 1992, 7, p.63.
4. Vinitsky S.I., Ponomarev L.I. — Sov. J. Part. Nucl., 1982, 13, p.557.
5. Ponomarev L.I., Puzynin I.V., Puzynina T.P. — JINR Report P4-8884, Dubna, 1975; J. Comp. Phys., 1976, 22, p.25.
6. Chiccoli C. et al. — IFNFN/BE-91/09 Bologna, 1991.
7. CVohen J.S., Struensee M.S. — Phys. Rev., 1991, A 41(7), p.3460.

Received on August 17, 1992.

УДК 539.123

THE EXPERIMENTAL POSSIBILITY OF MEASURING THE MAGNETIC MOMENT OF NEUTRINO UP TO 10^{-11} OF BOHR MAGNETON WITH A NEUTRINO SOURCE

O.A.Zaimidoroga

It is shown that neutrino magnetic moment can be sensitively investigated by neutrino-electron scattering using high intensity artificial neutrino source.

The investigation has been performed at the Particle Physics Laboratory, JINR.

Экспериментальные возможности измерения магнитного момента нейтрино до 10^{-11} магнетонов Бора от нейтринного источника

О.А.Займидорога

Исследования нейтрино-электронного рассеяния очень чувствительны к вкладу рассеяния, обусловленного магнитным моментом нейтрино. Показано, что магнитный момент нейтрино может быть измерен на подземной установке Борексино с помощью высокоинтенсивного искусственного источника нейтрино.

Работа выполнена в Лаборатории сверхвысоких энергий ОИЯИ.

The existence of magnetic moment of neutrino is already beyond the Standard Model (SM is QCD + electroweak theory). The leptons in SM are left-handed chirality. The alternative way to the SM is the generalisation of SM in a way to include a right-handed chirality states [1]. This leads for neutrino to have a magnetic moments and it does not depend on the neutrino having or having not a mass. Also there are the sensitivity to the type of neutrino:

— Dirac neutrino has a right-handed singlets and magnetic moment is proportional to the mass of neutrino;

— Majorana type of neutrino has no singlets and magnetic moment is equal to zero.

There are two experimental facts which are in the favour of the existence of magnetic moment of neutrino.

— Deficit of neutrino flux from the Sun.

— Anticorrelation of neutrino flux with the Sun activity.

If the solar neutrino flux is correlated with the solar cycle, the most viable scenarios advanced so far have built upon a large neutrino magnetic moment. The Standard Model predicts $\mu_\nu \sim 10^{-19} \mu_B$. For solar scenarios, values of the order of $10^{-11}\ \mu_B$ are desired. The discovery of such a moment would thus clearly compel new physics beyond the SM. Serious theoretical efforts are being made to explore new concepts leading to a large magnetic moment combined with a small neutrino mass [2,3,4]. At present, laboratory measurements limit the value of μ_ν less than $4 \times 10^{-10}\ \mu_B$.

The key points for the explanation of the experimental facts are the following. The passage of Dirac neutrinos with (diagonal) neutrino magnetic moment through distances of the order of the convection zone of the Sun in the presence of a magnetic field can induce a spin precession resulting in a right-handed neutrino. Since this object is normally considered sterile, hence undetectable at Homestake, a change in the neutrino flux would result. With a magnetic field correlated with the solar cycle, the neutrino flux could follow suit via this mechanism. A Majorana neutrino transition magnetic moment, with only off-diagonal elements, interacting with a solar magnetic field, converts both spin and flavor. This effect must therefore be considered in a coupled fashion with the MSW effect.

The implications of such a scenario are: a moment $\sim 10^{-11}\ \mu_B$ together with a magnetic field of $\sim 10^4$ gauss in the convection zone of the Sun and a field $\sim 10^6$ to 10^7 gauss in the center of Sun are necessary. This scenario is valid for $\Delta m^2 < 10^{-9}$ eV^2, thus, neutrino mass/mixing parameters or the MSW effect play no role.

Neutrino magnetic moments can be sensitively investigated by neutrino-electron scattering using a strong radioactive sources of antineutrinos and neutrinos. The presence of a magnetic moment adds a new component to the scattering cross-section.

Weak elastic antineutrino-electron scattering is

$$\frac{d\delta}{dT}(q) = \delta_0 \left[Q_i^2 + Q_r^2 \left(1 - \frac{T}{q}\right)^2 - Q_i Q_r \frac{m_e T}{q^2} \right],$$

where $\delta_0 = 88.3 \times 10^{-46}$ cm^2; $Q_i = \sin^2\theta_w$; $Q_r = \frac{1}{2} + \sin^2\theta_w$; m_e, mass of electron; T, recoil energy of electron; q, energy or antineutrino; θ_w, angle of Weinberg. For νe-scattering $Q_i = \frac{1}{2} + \sin^2\theta_w$ and $Q_r = \sin^2\theta_w$.

The electromagnetic cross-section is:

$$\frac{d\delta}{dT}(q) = \frac{\pi\alpha^2}{m_e^2}\mu_\nu^2\left(\frac{1}{T} - \frac{1}{q}\right),$$

where α is a fine structure constant.

The recoil electron spectrum rises rapidly at low energies unlike the flat profile of weak ν-e scattering, consequently, the cross-section is larger, the smaller the lower cut-off on the recoil energy. Furthermore, the recoil spectral profile in scattering provides a diagnostic magnetic signature by the $1/T$ dependence.

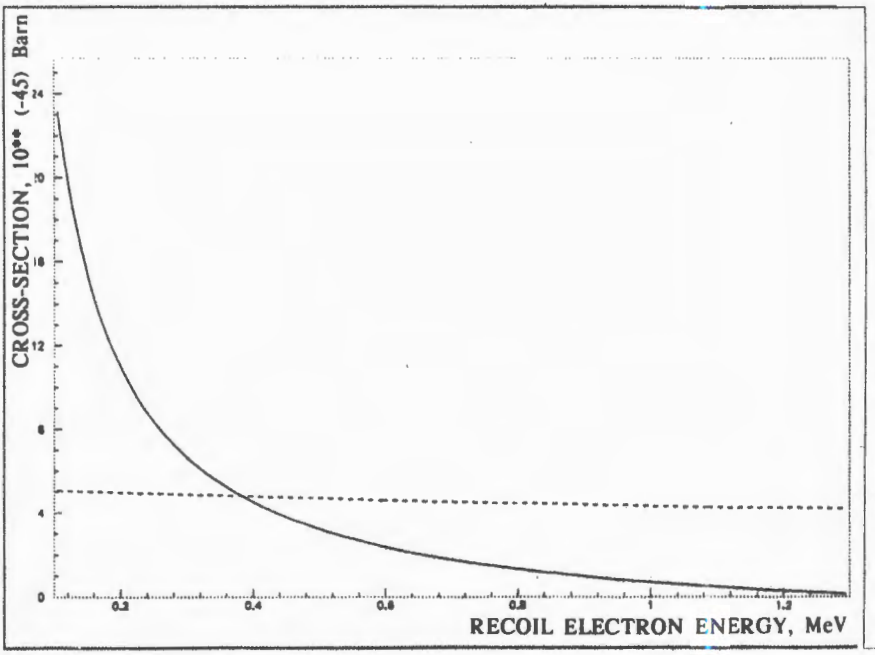

Fig.1. Electromagnetic and weak cross-section as a function of recoil electron energy

In Fig.1 the comparison of the weak and magnetic ν-e scattering cross-section with $\mu_\nu = 1.5 \times 10^{-10} \mu_B$ as a function of the electron recoil kinetic energy T is presented.

To detect such low energy recoil energy of electron we are going to use the Borexino detector at the Gran Sasso Underground Laboratories in Italy [5]. The Borexino will provide a high quality low-energy neutrino spectrometry with a low threshold ($\geq$ 0.2 MeV). We plan to investigate antineutrino-electron scattering using a laboratory radioactive source of $Sr^{90} - Y^{90}$, which emits antineutrino. The proposal to use a neutrino source to measure a magnetic moment of neutrino was presented in Singapore XXY Conference on High Energy Physics by R.Raghavanm P.Raghavan and the author [6]. With such a source the low energy scattering signal in Borexino also can be calibrated. A 1 *Mci* Sr^{90} source placed just outside the fiducial volume of detector will induce a signal of the same order as a Sun. Besides that an important advantage of the source measurement is its differential nature (source «on» — source «of») so that the background concerns are peripheral.

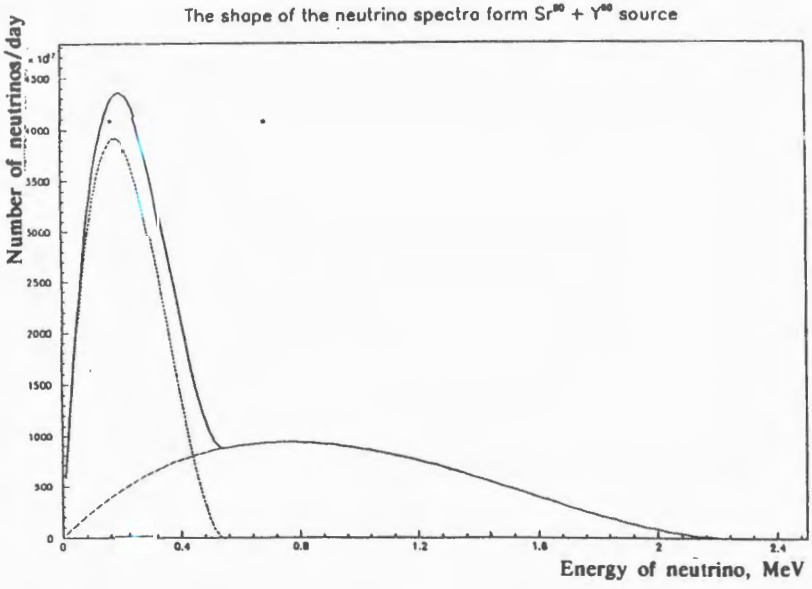

Fig.2. The neutrino spectrum from the $Sr^{90} - Y^{90}$ source. Dashed line is the activity after 1000 days

Sr^{90} ($T_{1/2} = 28\ y$, $E_{max} = 0.56$ MeV) and Y^{90} ($T_{1/2} \equiv 64\ h$, E_{max} + + 2.27 MeV) emit 2 $\tilde{\nu}e$'s/Sr decay at equilibrium. Both β^--decays are unique forbidden types with precisely calculable shapes. The $\tilde{\nu}$-spectrum from this source of 1 *Mci* is shown in Fig.2. The scattering cross-section averaged in the energy region 0.2 to 0.8 MeV (the usual low energy signal window in Borexino) is calculated to be equal to 21×10^{-46} cm^2. 1 *Mci* source ($10^{16}\ \tilde{\nu}$/sec) placed near fiducial volume (3.5 m from center of Borexino) can produce a $\tilde{\nu}e$ — signal of 72 events/day due to a weak interaction. With a half year's exposure, the $\tilde{\nu}e$ — cross-section can be measured to a precision of a few percent.

The presence of a magnetic moment of the order ~ 10^{-10} can be easily detected in Borexino.

The signal enhancement due to magnetic neutrino scattering as a function of μ_ν is shown in Fig.3. This curve indicates that with a precision of a few percent of the scattering cross section, an upper limit

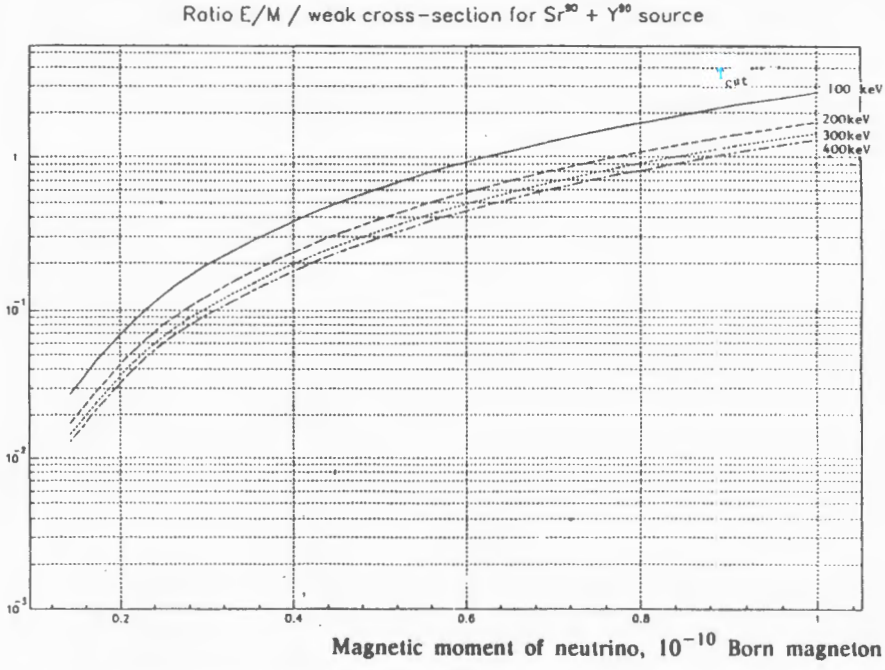

Fig.3. Enhancement of $\tilde{\nu}e$-scattering signal as a function of neutrino magnetic moment

of 2×10^{-11} can be set in Borexino. This value is by a factor of ten below the present limits.

So, in conclusion, using a neutrino source we will be able to estimate an electromagnetic scattering in $\tilde{\nu}e$-scattering, to put a limit for right-handed helicity states of neutrino.

From the detector's point of view the $\tilde{\nu}$-source would allow one to evaluate a background, to prove a convolution method of pattern recognition of ν-e events and to study a possible systematic errors.

References

1. Okun L.B., Voloshin M., Vysotski M. — Sov. Phys. JETP, 1986, 64, p.446.
   Babu K.S., Mohaparta R. — Maryland Report UMD-PP-91-100, 1990.
2. Voloshin M.B., Vysotski M. — Sov. H. Nucl. Phys., 1986, 44, p.564.
3. Vogel P., Engel J. — Phys. Rev., 1989, D39, p.3378.
4. Akhmedov E. — Sov. J. Nucl. Phys., 1988, 47, p.689.
5. Arpesella C. et al. — Proposal of Borexino, edited by Dept. of Physics of the University of Milano and Instituto Nazionale di Fisica Nucleare, August, 1991.
6. Proceedings of 25th High Energy Conference, Singapore, August, 1990.

Received on August 28, 1992.

УДК 539.1.074.2

THE PRELIMINARY STUDY OF PRESSURIZED DRIFT TUBES AS A DETECTOR FOR PRECISION MUON TRACKING

G.D.Alekseev, S.A.Baranov, Yu.E.Bonushkin, G.A.Shelkov, B.Fialovski, G.V.Karpenko, N.N.Khovansky, Z.V.Krumstein, V.L.Malyshev, Yu.V.Sedykh, V.V.Tokmenin

The pressurized cylindrical drift tubes are proposed as a detector for precision muon tracking. Such a detector is suitable where high individual coordinate accuracy (well below 100 microns) is needed and it helps to decrease remarkably a number of detecting layers. The preliminary results include an accuracy versus gas pressure dependence obtained with the system of stainless steel tubes of 0.2 mm wall thickness, 20 mm in diameter and 40 cm long operated in the self-quenching streamer mode, using Ar/CH4/C4H10–75/8/17 gas mixture.

The investigation has been performed at the Laboratory of Nuclear Problems, JINR.

Изучение дрейфовых трубок повышенного давления в качестве точного детектора для мюонных систем

Г.Д.Алексеев и др.

Цилиндрические дрейфовые трубки повышенного давления предложены в качестве точного детектора для мюонных систем. Такой детектор необходим в случае потребности в координатной точности лучше 100 микрон, он также позволяет значительно уменьшить число детектирующих слоев. Предварительные результаты включают зависимость разрешения от давления, полученную на системе трубок из нержавеющей стали с толщиной стенок 0,2 мм, 20 мм в диаметре и длиной 40 см, которые работали в самогасящемся стримерном режиме на газовой смеси Ar/CH4/CH10–75/8/17.

Работа выполнена в Лаборатории ядерных проблем ОИЯИ.

1. Introduction

The investigation of an accuracy versus gas pressure dependence was done with the system of stainless steel tubes 20 mm in diameter operating in self-quenching streamer mode at different voltages. The tubes were exposed at the electron beam of Serpukhov accelerator.

The main idea of the study is to measure the achievable coordinate accuracy with a tube of relatively large diameter. The results obtained with «straw» tubes [1] indicate that with small diameter (few mm) and

in streamer mode of operation one can improve accuracy with pressure roughly as $1/p$. At such a diameter the statistics of primary ionization has an important contribution to an accuracy. With increasing diameter (few cm) the diffusion plays increasing role and one could try to minimize it varying mode of operation, readout scheme, etc.

Coming from analogy with «straw» tubes let us call this detector "bamboo" tubes because of bigger diameter and more regidity.

This detector was proposed [2,3] as a good candidate for precise muon tracking for spectrometers with ironless muon systems.

The present study is performed following the JINR research plan item «Development of detectors for installation to be used with future colliders» and as a part of common R&D of Laboratory of Nuclear Problems JINR (Dubna) and Max Plank Institute (Munich) on precise muon tracking.

2. Experimental Setup

Bamboo tubes were 40 cm long, 20 mm in diameter with stainless steel wall 0.2 mm thick and gold-plated tungsten wire 50 microns in diameter, strung with 400 g. The chamber includes 4 parallel tubes, the forth one is shifted by 8 mm (fig.1). The tubes are blown in parallel from a common volume which also contains high voltage circuit.

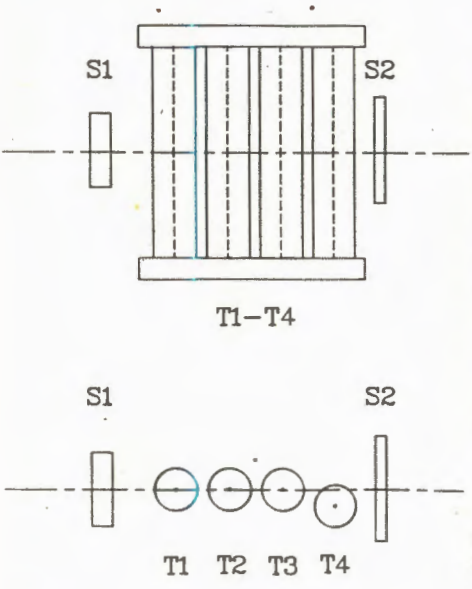

Fig. 1. Layout of setup: *T1—T4* are «bamboo» tubes, *S1—S2* are scintillators

The measurements were done making use of very high intensities 2*10**4 and 1*10**4 1/s per cm of anode wire for 10 and 15 GeV electron beam, respectively. Tracks were selected by coincidence of two scintillators and three unshifted tubes. XP1020 photomultiplier (S1) provided good timing signal for start in drift time measurements.

Tubes were operated in the self-quenching streamer mode with signal average amplitude ranged

from 50 to 150 mV on 50 Ohm impedance. Current preamplifiers we used had the gain equal to 20. After passing 50 m long cables the signals from 4 tubes and timing photomultiplier $S1$ were shaped (shaper threshold was set equal to 30 mV) and connected to the input of LeCroy TDC model 2228 A, which sensitivity was set equal to 170 psec/bin.

We used gas mixture Argon/Methane/Isobutane = 75/8/17 which provides an average drift velocity about 45 microns/ns.

3. Measurements and Results

We measured a spatial resolution at absolute pressures from 1 to 7 atm for several operation voltages (average signal amplitudes) at each point.

The value $(T1+T3)/2-T2$ was monitored during the run, where T is the drift time, as well as the correlation in time for different pairs of unshifted tubes. The typical correlation plot for drift times of two tubes is given in Fig.2.

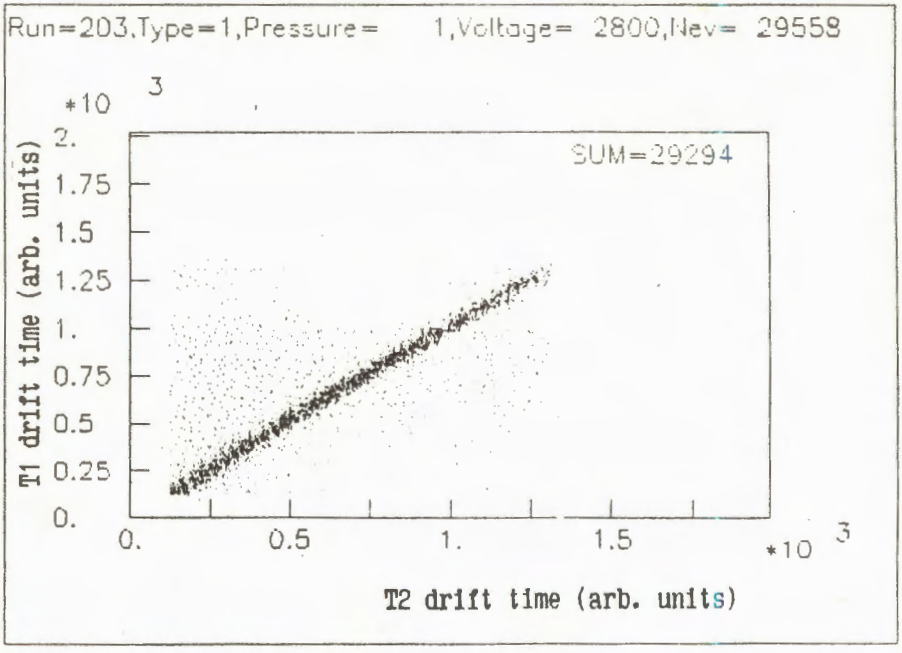

Fig. 2. Correlation plot of drift times for two tubes

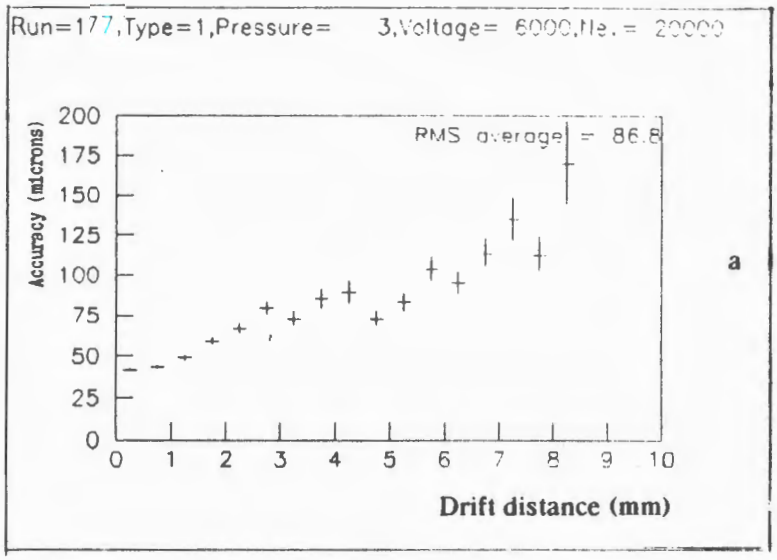

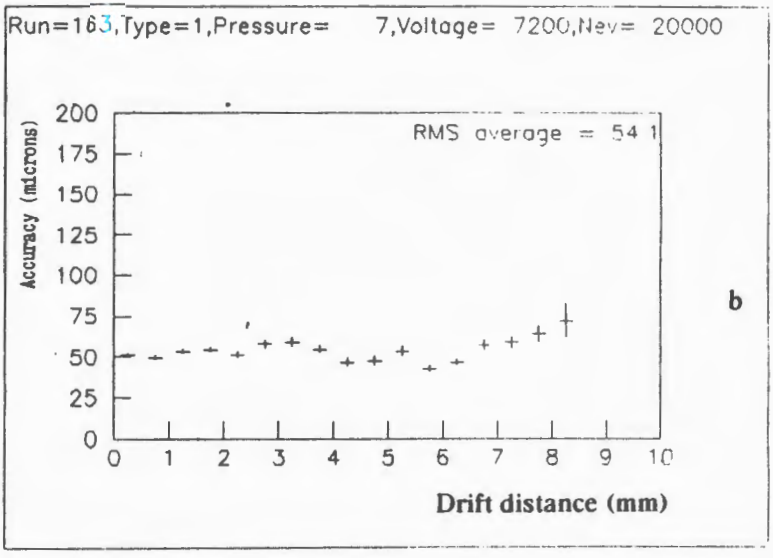

Fig. 3. Accuracy versus drift distance for 3 atm (a) and 7 atm (b)

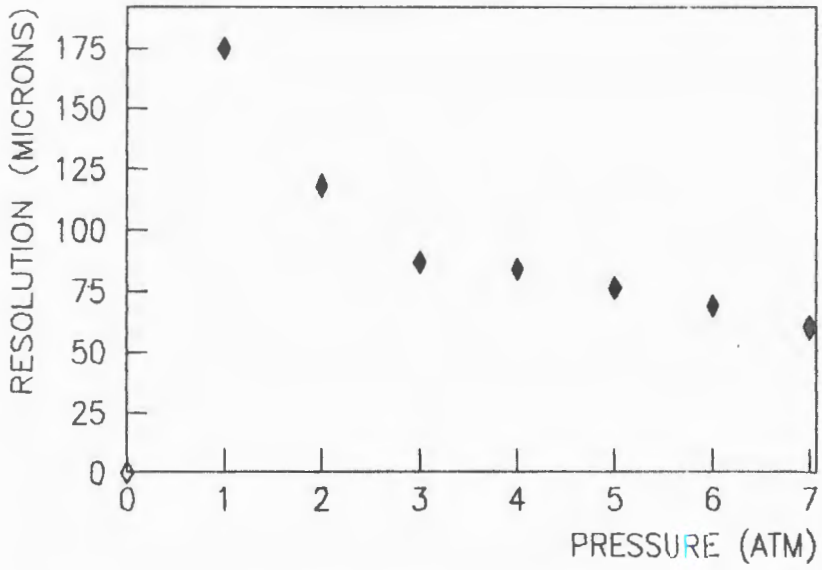

Fig. 4. Average resolution versus absolute pressure

To reject background events in off-line data processing we used simple algorithm: we took 2-dimensional plots of time correlations between the tubes 1 and 2, 1 and 3, 2 and 3 (which look like in fig.2) and rejected all bins with content less than 10% of maximal bin content.

The drift time-to-distance function was calculated for each meaning of pressure-voltage. For that we computed the convolution of drift velocity dependence on electric field [4] with field strength in cylindrical geometry.

Spatial resolution R of a single tube was obtained under assumption of equal accuracy of all tubes from expression:

$$R = \mathrm{sqrt}(2/3)*((r1 + r3)/2 - r2),$$

where «r» is the drift distance from track to the wire. As the beam was quasi-parallel to the axis of setup and had a small divergence (see correlation plot in fig.2) we could easily produce the dependence of spatial accuracy on drift distance. For that purpose the drift distance along the radius of the tubes was cut into small «slices» and for each slice quantity R was computed. An example of obtained spatial resolutions for 15 GeV electrons is presented in fig.3.

Figure 4 shows the behaviour of coordinate accuracy (averaged over the tube radius) with increasing pressure for 15 GeV electrons.

The above data (in figures 3 and 4) are given with voltages providing the best (minimal) mean spatial resolution after the voltage scan at different pressures.

We observed also a remarkable change of signal shape with pressure increase. The duration of signal (at 10% level of amplitude height equal roughly to 100 mV/50 Ohm) decreased from more than 200 ns at normal pressure to less than 50 ns at 8—10 atm. Being a known phenomenon it gives nevertheless an additional argument to the idea of pressurization as it minimizes an occupancy time per wire.

4. Conclusion

The spatial resolution below 100 microns was achieved with fast gas mixture and with tube of relatively big diameter for absolute pressures 2 atm and above. That resolution was obtained at very high counting rate, close to a counting rate limit in streamer mode, so we may hope for even better accuracy at normal conditions.

The resolution improves with pressure, which gives one a simple way to control a necessary level of coordinate accuracy of apparatus and to minimize the number of detecting layers.

Note, that such type of detector was chosen for precise muon tracking by the ASCOT project at LHC, and is being considered as a candidate for muon tracking in united ASCOT/EAGLE project at LHC, and in GEM collaboration at SSC. We expect this results to be of importance to our work on development of muon systems for the future colliders.

Further investigations are required to understand in detail the processes which influence the spatial resolution at high pressure.

The authors are grateful to F.Dydak of MPI (Munich) for support and providing a necessary equipment, and to V.Obraztsov, V.Lapin, A.Petrukhin and T.Lomtadze of IHEP (Protvino) for their help in beam measurements.

References

1. Ash W.W. et al. — NIM, 1987, A261, p.399.
2. Alekseev G.D. — EMPACT/TEXAS Note 230, June, 1990.
3. Ahlen S. — Report to GEM Collaboration, SSC Lab, June 1991.
4. Schultz G., Gresser J. — NIM, 1978, 151, p.413.

Received on August 17, 1992.

УДК 539.12.01

KINETIC EQUATIONS FOR THE QUARK CONDENSATE IN THE NJL TYPE MODELS

M.A.Kuptsov*, A.V.Prozorkevich, S.A.Smolyanskii*, V.D.Toneev

In the self-consistent mean field approximation, the Vlasov type kinetic equation is derived within a schematic four-fermion superconducting model of the Nambu — Jona — Losinio type for an arbitrary group of internal symmetry. The Eguchi — Sugawara equation is generalized to the case of finite temperature and density resulting in the Ginzburg — Landau type equation. Perspectives of the implementation of these kinetic equations for describing dynamics of the meson evolution in heavy ion collisions at relativistic energies are discussed.

The investigation has been performed at the Laboratory of Theoretical Physics, JINR and at the Saratov State University.

Кинетические уравнения для кваркового конденсата в моделях типа Намбу — Иона — Лазинио

К.А.Купцов и др.

В рамках схематической 4-фермионной сверхпроводящей модели типа Намбу — Иона — Лазинио для произвольной группы симметрии в приближении самосогласованного поля получено кинетическое уравнение Власова. Получено также уравнение типа Ландау — Гинзбурга, которое является обобщением уравнения Егучи — Сугавары на случай конечных температур и плотностей. Обсуждаются перспективы применения этих уравнений для описания динамики эволюции мезонов при столкновении тяжелых ионов в области релятивистских энергий.

Работа выполнена в Лаборатории теоретической физики ОИЯИ и Саратовском государственном университете.

A microscopic study of the dymanics of heavy-ion collisions is a central problem in the modern relativistic nuclear physics. In the last time much attention has been paid to the derivation of kinetic equations for describing the evolution of hot and compressed hadronic nuclear matter. These results are based mainly on the Walecka model but obtained by using a different technique [1]. A procedure to derive kinetic equations (KE) is not simple

*Physics Department, Saratov State University, Astrakhanskaya 83, 410071 Saratov, Russia

and, in this connection, the non-equilibrium statistical operator method introduced by D.N.Zubarev [2] has some advantage because it permits one to overcome a large part of the path of deriving KE in a very general form without any specification of the interacting system. Recently, the relativistic-invariant generalization of the Zubarev method has been carried out in paper [3], where within perturbation theory the quantum KE with collision integrals of the first and second order in the interaction coupling were obtained. In particular the KE for the baryonic sector of the Walecka model were considered and the collision integrals of the first (Vlasov's type) and second (Bloch's type) order were investigated in the slowly changing field approximation. Spin effects have been involved into consideration naturally. These results can be easily generalized to other kinds of interaction with vertices of the 'three-tails" type and it has been done in [3] for the case of chiral symmetry theory.

In this paper we shall take the method of ref.[3] as a starting point for deriving the KE of Vlasov's type for the quark condensate within the Nambu — Jona — Losinio (NJL) type models at finite temperature and density. As the first step, we consider the simplest version of the NJL model with the only kind of fermions and with chiral and translational symmetry breaking, the so-called Eguchi — Sugawara version of the NJL model [4]. The more realistic quark SU(N) NJL model which may serve as an approximation of QCD in the long-wave length limit will be discussed in other paper. It is noteworthy that in the original paper [5], the translation symmetry theory at zero temperature has only been considered. The extension of the NJL model to the case of non-zero temperature can be find in papers [6]—[9]. The Eguchi — Sugawara model [4] takes into account both chiral and translational symmetry breaking but at zero temperature. In the present paper this version of the NJL type models will be extended to temperatures different from zero.

The initial Lagrangian density of the NJL type model with two kinds of the coupling constants has the following form [4]:

$$(x) = \overline{\psi} i\gamma \nabla \psi + g\,[(\overline{\psi}\psi)^2 - (\overline{\psi}\gamma_5\psi)^2] - g'\,[(\overline{\psi}\gamma_n\psi)^2 + (\overline{\psi}\gamma_5\gamma_n\psi)^2].$$

In the Hartree — Fock approximation, we get from here the Eguchi — Sugawara Lagrangian density

$$_{ES}(x) = \overline{\psi}(x)\,[i\gamma - \hat{m}(x)]\psi, \qquad (1)$$

where

$$\hat{m}(x) = m^S(x)I + i\gamma_5 m^P(x) + \gamma^n m_n^P(x) + \gamma^n m_n^V(x) + \gamma_5\gamma^n m_n^A(x),$$

$$m^S(x) = -2g\, Sp\, \langle \bar{\psi}(x)\psi(x) \rangle_\tau ,$$

$$m^P(x) = -2ig\, Sp\, \gamma_5 \langle \bar{\psi}(x)\psi(x) \rangle_\tau ,$$

$$m_n^V(x) = (4g' + g)\, Sp\, \gamma_n \langle \bar{\psi}(x)\psi(x) \rangle_\tau ,$$

$$m_n^A(x) = (4g' - g)\, Sp\, \gamma_5\gamma_n \langle \bar{\psi}(x)\psi(x) \rangle_\tau . \qquad (2)$$

Unlike ref.[4], the averaging in these expressions is performed by using the non-equilibrium statistical operator $\rho(\tau)$, i.e. $\langle \dots \rangle_\tau = Sp \dots \rho(\tau)$. This operator introduces the local temperature $T(x)$ in this model. Equations (2) define a set of the non-equilibrium order parameters of the theory which are considered as a measure of the chiral symmetry breaking.

Formally, the Lagrangian density (1) corresponds to the quasi-free motion of a particle with the translation non-invariant «mass» matrix $\hat{m}(x)$. According to eq.(1), the quadrical equation of motion is given by ($f_{,n} \equiv \partial f(x)/\partial x^n$)

$$\{\nabla^2 - i\gamma^n \hat{m}_{,n}(x) - [\gamma^n, \hat{m}(x)]\nabla_n - \hat{m}^2(x)\}\, \psi(x) = 0. \qquad (3)$$

Following ref.[3] and taking into account this quasi-free motion equation, the general KE can be written down in the approximation (2) as follows

$$p^n \frac{\partial}{\partial x^n} f_{\alpha\beta}(x, p) = -i\sqrt{p^2}\,(2\pi)^{-4} \int d^4y\, e^{-ipy} \times$$

$$\times \langle [\bar{\psi}_\beta(x + y/2)\, \psi_\alpha(x - y/2), H_{ES}] \rangle_\tau . \qquad (4)$$

Here the Hamiltonian H_{ES} corresponds to the Lagrangian density (1) for the Eguchi — Sugawara model and $f_{\alpha\beta}(x, p)$ is the relativistic Wigner function

$$f_{\alpha\beta}(x, p) = (2\pi)^{-4} \int d^4y\, e^{-ipy} \langle \bar{\psi}_\beta(x + y/2)\, \psi_\alpha(x - y/2) \rangle_\tau . \qquad (5)$$

Keeping the first order terms in coupling counstants in eq.(4), one can get the resulting KE of the Vlasov type in the Wigner representation, to be nonlocal equation for (5). In the long-wave approximation, it reads:

$$p^n \frac{\partial f}{\partial x^n} = \frac{1}{4}\{f, \{\hat{m}_{,n}, \gamma^n\}\} + \frac{i}{2}\{f, [\hat{m}, p\gamma]\} - \frac{1}{4}[\frac{\partial f}{\partial p_n}, [\frac{\partial \hat{m}}{\partial x^n}, p\gamma]] -$$

$$- \frac{1}{4}\{\frac{\partial f}{\partial p_n}, \frac{\partial \hat{m}^2}{\partial x^n}\} + \frac{1}{4}[\frac{\partial f}{\partial x^n}, [\hat{m}, \gamma^n]] + \frac{i}{2}[f, \hat{m}^2]. \qquad (6)$$

Here the order parameters (2) can be expressed through the Wigner function (5)

$$m_a(x) = Sp\,\Gamma_\alpha \int d^4p\, f(x, p), \qquad (7)$$

where the index enumerates the order parameters from the set (2). The matrix Γ^α consists of a combination of corresponding coupling constant and γ-matrices. So, the correlations (7) mean that the KE (6) is a system of nonlinear integro-differential equations for the Wigner function and its zero moments.

Discussing the final KE (6), one should note that the system under consideration will be translationally invariant at thermodynamical equilibrium. This leads to the following requirement for the equilibrium Wigner function $f^{(0)}$:

$$[f^{(0)}, \hat{m}^2_{(0)}] + \{f^{(0)}, [\hat{m}_{(0)}, p\gamma]\} = 0. \qquad (8)$$

The matrix structure of the equilibrium order parameter is defined in ref. [9]: $\hat{m}_{(0)} = m_T I + \delta\mu\gamma^0$, where $\delta\mu$ is the chemical potential correction and m_T is the scalar mass at finite temperature. We have $m_T \to m_\infty$ at $T \to 0$, where m_∞ is the mass of a condensate boson in the NJL model at $T = 0$. The last relation for the $\hat{m}_{(0)}$ agrees with a general structure of the Wigner $f^{(0)} = \alpha I + b_n\gamma^n$ function [10]. After substitution of $\hat{m}_{(0)}$ and $f^{(0)}$ into eq.(8) we get the equality $a = b$ assuming $b_n = b(p)p_n$. Below we shall consider a simpler case when there is no vector fields, which results in the zero changing of the chemical potential in the equilibrium state, $\delta\mu = 0$.

In this case it is possible to derive a closed system of equations for weakly non-equilibrium order parameters $\delta\hat{m} = \hat{m} - \hat{m}_{(0)}$. Let us assume that $\delta f(x, p) = f(x, p) - f^{(0)}(p)$ is also small and substitute $\delta\hat{m}$ and $\delta f(x, p)$ into eq.(6) restricting ourselves by linear terms for small deviations from an equilibrium state. After carrying out the Fourier

transformation, we arrive at the following system of equations for non-equilibrium order parameters:

$$\delta m_a(k) = \frac{1}{2} Sp \int d^4p \frac{\Gamma_a}{pk} (\frac{1}{2} \{f^{(0)}(p), \{\delta\hat{m}(k), k\gamma\}\} -$$

$$- \{f^{(0)}(p), [\delta\hat{m}(k), p\gamma]\} - \frac{1}{2} [k \frac{\partial f^{(0)}(p)}{\partial p}, [\delta\hat{m}(k), p\gamma]] -$$

$$- m_T \{k \frac{\partial f^{(0)}(p)}{\partial p}, \partial\hat{m}(k)\} - 2m_T [\partial\hat{m}, f^{(0)}(p)]). \qquad (9)$$

These equations can be considered as a certain analogy of the gap equations for the non-equilibrium state.

The initial model Lagrangian is independent of internal symmetry of fields involved. So, the KE (6) and (9) based on this Lagrangian are valid for any SU(N) version of the NJL model. In this sense the above-derived KE (6) and (9) can be considered as generalized KE. In particular, the vector meson degrees of freedom in (x) may be eliminated by the Fierz transformation.

The Vlasov type KE (6) is reasonable in the self-consistent field approximation. It is not very hard to get the collision integral of the Bloch type to be second order in the coupling constant (see ref.[3]). It is noteworthy that in this case a quasiparticle scattering should be expressed in terms of «residual» interaction, i.e. for the Lagrangian $_{in} = _{in} - \bar{\psi}\hat{m}\psi$. By constructing $\hat{m}$, we have $\langle _{in} \rangle_{in}$ in the Hartree — Fock approximation.

In this sense, a free motion is not yet a foundation of the perturbation theory in the NJL type models. However, it does be so when considered with the Lagrangian density (1). In this case the mass shell equation is given by $p^2 = m_T^2$ and depends on $T(x)$.

Eq.(6) describes the kinetic stage of the system evolution when a fast motion is eliminated from consideration. However, the exact equation of motion for the Wigner function (5) can be derived by means of the method of ref.[11]. In the Hartree — Fock approximation for (1), it results in the following equation:

$$\gamma^n (p_n + \frac{i}{2} \frac{\partial}{\partial x^n}) f(x, p) = \exp(-\frac{1}{2} \frac{\partial}{\partial x^n_{(m)}} \frac{\partial}{\partial p_n}) \hat{m}(x) f(x, p). \qquad (10)$$

The sign (m) means that the operator $\partial/\partial x^n_{(m)}$ acts only on the matrix $\hat{m}(x)$. It is of interest that eq.(10) may serve as a basis for deriving a closed system of wave equations in fields (7). These equations are a

straightforward generalization of the Eguchi — Sugawara wave equations for the case of finite temperature. In the limiting case $\mu \to 0$ and $T \to 0$ we have $\mu_T \to \mu_\infty$ and our equation of the Ginzburg — Landau type is reduced to that of ref.[4].

Eqs.(6), (9) and (10) may be used for extracting the information of various kinds about a meson subsystem of nuclear matter. So, their solution for the Wigner function can provide the canonical kinetic description of «bozonized» quark systems (as well as hydrodynamical description, problems of the proper frequency and decrement constants etc.). Particularity of this description is the presence of the order parameters $\hat{m}(x)$. In some cases, it is possible to write down a closed system of equations for bosonic degrees of freedom without any reference to a fermionic subsystem. Therefore, eqs.(6), (9) and (10) seem to be quite promising for the description of dynamical phase transition of the chiral symmetry restoration in a bosonic subsystem and for the study of meson properties in hot and dense nuclear matter.

References

1. Botermans W., Malfliet R. — Phys. Reports, 1990, 198, p.115.
2. Zubarev D.N. — Non-Equilibrium Statistical Thermodynamics. N.-Y., Consultant Bureau, 1974.
3. Erokhin S.V., Prozorkevich A.V., Smolyanskii S.A., Toneev V.D. — Theor. and Math. Physics, 1992, 91, p.346.
4. Eguchi T., Sugawara H. — Phys. Rev., 1974, 10D, p.4257.
5. Nambu Y., Jona-Losinio G. — Phys. Rev., 1961, 122, p.345.
6. Hatzuda T., Kunihiro T. — Phys. Rev. Lett., 1985, 55, p.155; Phys. Lett. B, 1987, vol.185, p.304; Progr. Theor. Phys. Suppl., 1987, 91, p.284.
7. Bernard V., Meisser U.-G. — Phys. Rev., 1988, 38, p.1551; Nucl. Phys., 1988, 489A, p.647.
8. Heley E.M., Muther H. — Nucl. Phys., 1990, 513A, p.667.
9. Vogl U., Weise W. — Progr.— Part. and Nucl. Phys., 1991, 27, p.667.
10. Hakim R. — Revista Nuove Cim., 1978, 1, p.1; Phys. Rev., 1978, 18A, p.1250.
11. Elze H. — Th. et al. — Mod. Phys. Lett., 1987, 2A, p.451.

Received on August 18, 1992.

УДК 539.12

THE OBSERVATION OF THE HEAVY STABLE POSITIVELY CHARGED $\tilde{H}^+$ (S= −2) DIBARYON

B.A.Shahbazian, T.A.Volokhovskaya, A.S.Martynov

We have succeeded in observing an event which is unambiguously interpreted as the weak decay of the heavy stable positively charged $\tilde{H}^+$ ($S=-2$) dibaryon. Its mass, equal to $M_{\tilde{H}^+} = (2377.5 \pm 9.5)$ MeV/c² is in fair agreement with the masses of the two heavy stable ($S=-2$) neutral dibaryons, (2408.9 ± 11.2) and (2384.9 ± 31.0) MeV/c², recently found.

The investigation has been performed at the Laboratory of High Energies, JINR.

Наблюдение тяжелого стабильного, положительно заряженного $\tilde{H}^+$ ($S=-2$) дибариона

Б.А.Шахбазян, Т.А.Волоховская, А.С.Мартынов

Нам удалось обнаружить событие, которое однозначно интерпретируется как слабый распад тяжелого стабильного, положительно заряженного $\tilde{H}^+$($S=-2$) дибариона. Масса его, равная $M_{\tilde{H}^+} = (2377{,}5 \pm 9{,}5)$ МэВ/с², находится в хорошем согласии с массами двух недавно найденных тяжелых стабильных ($S=-2$) нейтральных дибарионов, (2408,9 ± 11,2) и (2384,9 ± 31,0) МэВ/с².

Работа выполнена в Лаборатории высоких энергий ОИЯИ.

Recently we have reported [1,2,3] on two events, found on photographs of the JINR 2m propane bubble chamber exposed to 10 GeV/c proton beam of the Synchrophasotron, which were interpreted as the production and weak decays of the heavy neutral stable $\tilde{H}$ ($S=-2$) dibaryons of masses (2408.9 ± 11.2) and (2384.9 ± 31.0) MeV/c², coinciding with each other within the limits of errors. Moreover, the masses of these two events are very close to the lowest state of $S=-2$ dibaryons, $I=1, J^{\pi}=0^+$, $\{f\}=\{10^*\}$ stable with respect to strong decays of a mass 2370 MeV/c², predicted by the Callan — Klebanov — Kunz — Mulders soliton Skyrme-like model [4].

Fortunately, the propane bubble chamber technique makes it possible to search for all the three charge triplet components simultaneously, via weak decay modes

$$\widetilde{H}^+ \to p + \Lambda, \qquad \Lambda \to p + \pi^- \qquad (1)$$

$$p + \Lambda + \pi^0, \qquad \Lambda \to p + \pi^- \qquad (2)$$

$$p + \Lambda + \pi^+ + \pi^-, \qquad \Lambda \to p + \pi^- \qquad (3)$$

$$p + p + K^-, \qquad (4) \text{ etc.}$$

$$\widetilde{H} \to p + \Sigma^-, \qquad \Sigma^- \to n + \pi^- \qquad (5)$$

$$\widetilde{H}^- \to p + \Lambda + \pi^- + \pi^-, \qquad \Lambda \to P + \pi^- \qquad (6) \text{ etc.}$$

Therefore we have started with the search for the charged heavy stable dibaryons in the sample of events, compatible with the topologies (1) — (4).

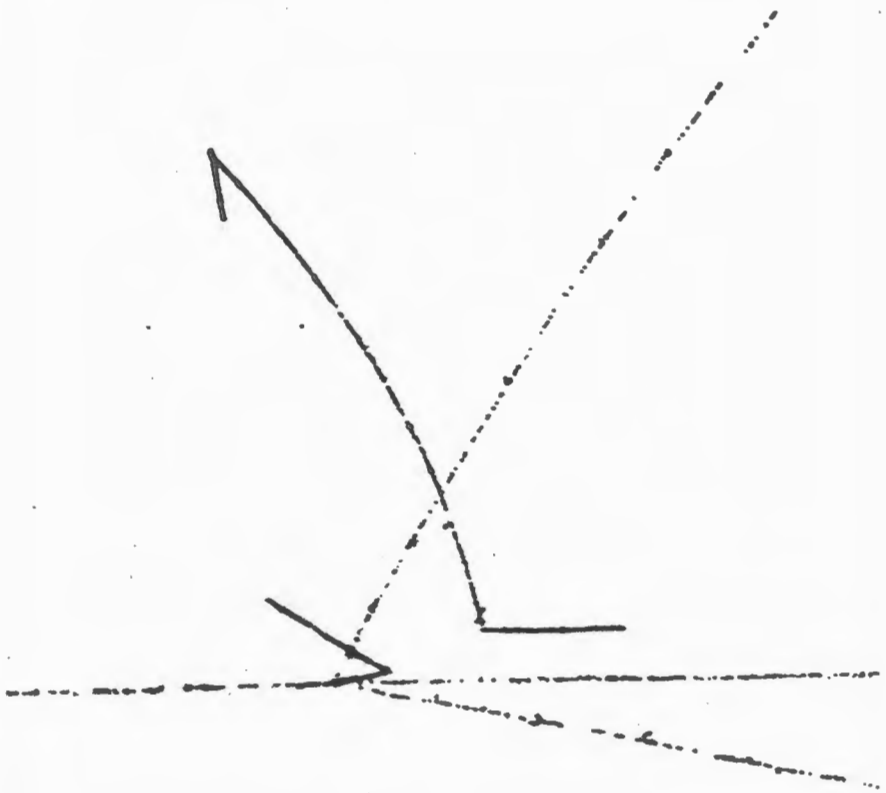

The $\widetilde{H}^+$ dibaryon suffering weak decay $\widetilde{H}^+ \to p + \Lambda + \pi^0$, $\Lambda \to p + \pi^-$

On the 10th of January 1992 a noteworthy event was found in this sample (Figure). A beam proton produces a four-prong star of a total electric charge $Q = +4$. The most intriguing in this star is the black kinked track. The appearance of its first part, 1.14 cm long, situated between the star and the kink — vertices, suggests that it is due to a very slow heavily ionizing positively charged massive particle, suffering violent scattering in propane. The second part is certainly due to a slow proton, $p_p = (261.5 \pm 5.7)$ MeV/c, which stops in propane. A slow V^0-particle is clearly seen near the star. The black track of the positively charged decay particle is due to a slow proton of $p_p = (259.7 \pm 5.8)$ MeV/c momentum, which stops in propane. The second decay track is due to a slow negative pion of $p_{\pi^-} = -(100.8 \pm 2.2)$ MeV/c, which also stops in propane, is captured by a carbon nucleus, which de-excitates, evaporating two short-range protons. Thus, the V^0 can be due to the weak decay of a lambda-hyperon only. Indeed, the invariant mass of the (p, π^-) pair is (1114.5 ± 1.5) MeV/c^2. The hypothesis on emission of this lambda from the primary interaction vertex fails to fit the event with $\chi^2(1\,V - 3\,C) = 50.4$. This negative result is due to a large noncoplanarity angle, $\eta = (0.36312 \pm 0.03254)$ radians, formed by the supposed line of flight, connecting the interaction and decay vertices, with the decay plane. Contrary to this, the hypothesis on emission of the lambda hyperon from the kink-vertex fits well the event with $\chi^2(1V - 3C) = 2.92$, C.L.= 40.5%, $p_\Lambda = (263.4 \pm 6.1)$ MeV/c. The proton and negative pion transversal momenta $p_p = (97.4 \pm 4.5)$ and $p_{\pi^-} = -(98.2 \pm 5.0)$ MeV/c coincide within the limits of errors.

Thus there arized the problem of the identification of the very slow massive particle able to produce two baryons, a lambda hyperon and a proton, at least. It should be noted that the best measurement of its momentum for the proton hypothesis was performed with a relative error of 80%. There are measurements, also with large errors, ascribing negative charge to the particle, e.g. $p_{K^-} = -(101.7 \pm 98.6)$ MeV/c for the K^--hypothesis. Therefore we had to examine all possible imitating reactions induced by both positively and negatively charged particles.

(i) Of all very slow positively charged particles only the Σ^+ hyperon is able to create a lambda hyperon and a proton. The hypothesis on the reaction sequence $\Sigma^+ + n \to \Lambda + p$, $\Lambda \to p + \pi^-$ failed to fit the event with $\chi^2\,(2V - 6C) = 645.8$. Here one has only two unmeasurable

parameters, the Λ and Σ^+ momenta. There were no (2V—4C) fits for the hypotheses on the reaction sequences $\Sigma^+ + n \to p + \Lambda + \pi^0$, $\Lambda \to p + \pi^-$ and $\Sigma^+ + (2n) \to p + \Lambda + n$, $\Lambda \to p + \pi^-$, $M(2n) = 2M_n$, as well.

(ii) No successful (2V—4C) fits of the reactions

$$K^- + (2p) \to p + \Lambda + \pi^0, \quad \Lambda \to p + \pi^-, \quad M(2p) = 2M_p$$

$$K^- + (2pn) \to p + \Lambda + N^0/\Delta^0, \quad \Lambda \to p + \pi^-, \quad M(2pn) = 2M_p + M_n$$

$$\Sigma^- + (2p) \to p + \Lambda + N^0/\Delta^0, \quad \Lambda \to p + \pi^-, \quad M(2p) + 2M_p$$

have been obtained. By N^0 and Δ^0 the neutron and all known neutral N- and Δ-baryons are meant.

(iii) The only alternative remains the hypothesis on weak decay modes of a positively charged stable dibaryon. The hypothesis on two-body weak decays $\widetilde{H}^+ \to p + \Lambda$, $\Lambda \to p + \pi^-$ failed to fit the event with $\chi^2(2V—6C) = 95.9$.

Only the hypothesis on the three-body weak decay $\widetilde{H}^+ \to p + \Lambda + \pi^0$, $\Lambda \to p + \pi^-$ fits well the event with $\chi^2(2V—3C) = 3.24$, C.L. = 35.6%.The best-fit parameters are: $M_{\widetilde{H}^+} = (2377.5 \pm 9.5)$ MeV/c^2, $p_{\widetilde{H}^+} = (50.0 \pm 40{,}6)$ MeV/c, $\mathrm{tg}\,\alpha_{\widetilde{H}^+} = 0.47661 \pm 0.27837$, $\beta_{\widetilde{H}^+} = (1.93508 \pm 0.12774)$ radians. Here $\alpha_{\widetilde{H}^+}$ and $\beta_{\widetilde{H}^+}$ are the dip and azimuthal angles, respectively. The large errors are due to the violent scattering of $\widetilde{H}^+$ in propane.

Finally, one cannot exclude that the weak decay $\widetilde{H}^+ \to p + \Lambda + \pi^0$ took place at rest. In this case one is deprived of the possibility of performing the kinematical fit except the (1V-3C) fit on $\Lambda \to p + \pi^-$ hypothesis. Then, using the fitted parameters of the lambda and four constraint equations, one can compute the mass of the $\widetilde{H}^+$ dibaryon and the three components of the neutral pion momentum. The mass obtained in this way, $M_{\widetilde{H}^+} = 2378.2$ MeV/c^2 is in excellent agreement with the above cited value.

Our attempts to perform exclusive multivertex kinematical analysis of the production (both on a proton and multibaryon targets) and the weak decay of the $\widetilde{H}^+$, were not successful. We ascribe this failure to the obscuring effect of the nuclear cascade process. In the recent article [3] we arrived at the conclusion, that both the heavy ($M_{\widetilde{H}} \sim 2M_\Sigma$) and light

($M_H < 2M_\Lambda$) dibaryons with the accompanying two kaons of $S = +1$ strangeness have appeared as a result of the phase transition of the nonstrange quark-gluon plasma (QGP) formed in the moment of the collision of 10 GeV/c protons with carbon nuclei. Thus the stable dibaryons serve as signatures of the QGP.

This new mechanism of the stable dibaryon formation fits well our empirical hypercharge selection rule: «The hypercharge of free hadrons (the exotic ones including) cannot exceed unity: $Y \leq 1$» ([5] and the earlier papers cited therein).

Now, it should be noted, that the quite unsufficient precision of the contemporary methods of the time interval measurement ($\Delta t = 9.11^{-11}$ s) do not permit one to discriminate the creation of the H ($\sim 10^{-22}$ s) against the substantial background of K^+-mesons produced together with hyperons or antikaons in nuclear cascade processes ($\sim 10^{-22}$ sec). This circumstance depreciates the tagging by the $K^- \to K^+$ strangeness exchange ($\Delta S = +2$) process, used in the experiments [6,7]. Therefore the reliable identification of the weak decay of the stable dibaryons H, $\widetilde{H}^+$, $\widetilde{H}$, $\widetilde{H}^-$ — turns into a problem of paramount importance. The urgency of this statement becomes quite evident for the production of dibaryons via phase transition mechanism, for the realization of which the collisions of relativistic ions with nuclei are best suited. But the backgrounds of any kinds, the K^+ mesons including, due to nuclear cascade and fragmentation processes are the highest possible ones in this case, as well. Therefore we are doomed to scrupulous multivertex kinematical analysis of a candidate for stable dibaryon weak decay observed, like the one, developed in [1,2,3] and this article. And the more dense is the material of the detector used (propane, fibre scintillators, nuclear emulsions), the more imperative is the necessity of such an analysis, irrespective of the projectile used.

Thus we have succeeded in observing an event of weak decay of a heavy stable positively charged dibaryon, $\widetilde{H}^+ \to p + \Lambda + \pi^0$, $\Lambda \to P + \pi^-$, of a mass $M_{\widetilde{H}^+} = (2377.5 \pm 9.5)$ MeV/c^2. This value within the limits of errors coincides with the masses of two neutral heavy dibaryons (2408.9 ± 11.2) [2] and (2384.9 ± 31.0) MeV/c^2 [3], observed earlier. For the present, at the cited errors one cannot speak of electromagnetic mass splitting. The mass, averaged over the three events, is (2390.4 ± 17.2) MeV/c^2, i.e. $\sim 2M_\Sigma$. The formally estimated effective cross section of the $\widetilde{H}^+$ production in $p^{12}C$ collisions at

10 GeV/c is 100 nb. The time of flight before the weak decay of the $\widetilde{H}^+$ is $1.8 \cdot 10^{-9}$ s.

Of all $\widetilde{H}^+$ weak decay modes (1)—(4) the simplest topology belongs to the mode (4). Note, that within the limits of errors $M_{\widetilde{H}^+} = M_{K^-} + 2M_p$. Then the laboratory proton and K^--meson momenta are $p_p = M_p(\beta\gamma)_{\widetilde{H}^+}$ and $p_{K^-} = M_{K^-}(\beta\gamma)_{\widetilde{H}^+}$. The weak decay via this mode would look out as a narrow trident with the radius of curvature of the K^- trajectory in a magnetic field equal to $R_{K^-} = (M_{K^-}/M_p) R_p$.

Perhaps this decay mode is best suited for the counter experiments with live targets. But even in this case for an unambiguous identification of the $\widetilde{H}^+$ one needs for either (1V—3C) or (2V—4C) kinematical analysis, depending on coordinates (the K^- momentum) of the K^- decay vertex. The search for H, $\widetilde{H}^+$, $\widetilde{H}$, $\widetilde{H}^-$-dibaryons is in progress.

References

1. Shahbazian B.A., Sashin V.A., Volokhovskaya T.A., Martynov A.S., to appear in Proceedings of the Int. Conf. "Hadron'91".
2. Shahbazian B.A., Volokhovskaya T.A., Martynov A.S. — JINRRapid Communications, No.3(54)-92, Dubna, 1992, p.38.
3. Shahbazian B.A., Volokhovskaya T.A., Martynov A.S. — JINR Rapid Communications, No.3(54)-92, Dubna, 1992, p.51.
4. Dover C.B. - Nuovo Cim., 1989, 102A, p.521; Callan C.G., Klebanov I. — Nucl. Phys., 1985, B262, p.365; Kunz J., Mulders P.I.D. — Phys. Lett., 1988, B215, p.449.
5. Shahbazian B.A. et al. — Z. Phys., 1988, C39, p.151.
6. Aoki S. et al. — Phys. Rev. Lett., 1990, 65, p.1729.
7. Imai K. — Talk at Int. Symp. on Hypernuclear and Strange Particle Physics, Shimoda, Japan, December, 1991.

Received on July 14, 1992.